

School of Physics and Astronomy



Evolution of Metabolic Networks MPhys Project Report

Balint Borgulya
21th March 2016

Abstract

The abstract is a short concise outline of your project area, **of no more than 100 words.**

Signature:

Date:

Supervisor: Dr. Bartek Waclaw

Contents

1	Introduction	4
1.1	Metabolic networks as graphs	5
1.2	Evolution	6
1.3	The chemistry of the problem???	7
1.4	Evolution in the eyes of a physicist	8
2	Methods	9
2.1	Anatomy of the organisms simulated	9
2.2	Calculating the free energy change	11
2.3	In silico Evolution	13
2.4	Flux Balance analysis	14
2.5	Data analysis	18
2.6	Technical remarks	19
3	Results	20
3.1	The effect of mutation rate	26
3.2	Multiple sources	31
3.3	The effect of objective functions	33
4	Discussion	38
4.1	Limitations of our approach	40

Personal statement

I spent the first two weeks reading literature suggested by my supervisor, and getting familiar with C++, as I have not worked with it before. I started developing the simulation software in early October. I originally used Boost Graph Library objects to store the reaction network, this way I could simulate simple trial networks at the end of October. It became apparent then that the functionality provided by Boost comes at a large performance cost, so in the first few weeks of November I restructured the program to use vectors and custom data structure to link reactions and substrates instead of the ones provided by Boost. I later implemented a pre-calculation of the reaction neighbour-list substantially speeding up the calculation. In the last week of November I implemented outputting the reaction networks into the XGMML file format that Cytoscape can read for visualisation of the networks.

Over the winter break I attempted creating an algorithm that would execute a Depth first search through all reactions in order to find alternative pathways to start the MN from, unfortunately this was very ineffective, so I used a subsection of normal glycolysis as the initial network. Over the break I also read articles in the field and I started drafting the report itself.

In January I started running the first simulations with the modified trunk of the glycolytic pathway as the initial network. I also implemented the scripts necessary to perform parallel simulations on multiple computers in the physics cplab, and collecting the results of these simulations. As the simulation results started to flow in, I started to create analysis tools for them, plotting relevant quantities. The format of the log file the simulation outputs while running changed and expanded during this time as additional summary statistics were added to it.

In February I changed the algorithm to use index-based cell types in the population population, where instead of 100 metabolic networks I only store 100 references to types of metabolic networks. This was a performance boost for the simulations with a low mutation rate, as the iterations when no mutations happened could be calculated nearly instantly, since the flux balance analysis problem wasn't necessary to solve in these cases.

In February and March I run into problems with the IT infrastructure at the simulating machines, slowing down the progress. I have also had simulations that were started with bad parameters. These errors were fixed when discovered.

I started writing the report in January, and worked on it continuously, however the majority of the work on it was done in March.

The project's GitHub page [5] and the commit history there serves as diary of the project.

Definitions

Metabolite: a chemical compound produced in the metabolic network.

Nutrient: chemical compound(s) a cell consumes in order to provide itself with energy and materials.

Enzyme: biological catalyst molecules, can lower the activation energy of a reaction therefore increasing the flux through that reaction.

ATP - Adenosine triphosphate: the energy currency molecule of cells, has 3 phosphate groups. Energy is released when converting ATP to ADP (removing a phosphate group), and can be stored by converting ADP to ATP (adding a phosphate group).

ADP - Adenosine diphosphate: key molecule in the cell's energy management, has one less phosphate group than ATP.

DNA - Deoxyribonucleic acid: the molecule carrying the genetic information required for reproduction and functionality of most living organisms and some viruses. Most DNA molecules (such as the human DNA) form the well known double helix.

Gene: a proportion of the DNA encoding a certain function of the cell (in our case the ability to perform a certain reaction).

Population: a set of cells competing and breeding in the same environment.

Generation: Natural unit of time for a population. A generation is the time it takes for N reproductions to take place in a population of N cells (on average every cell reproduces once).

Flux: (through a reaction): the rate — on an arbitrary scale — at which the given reaction converts its reactants to the products. It is usually denoted by v .

Allele: a variant of a certain gene. In our case an allele is the existence (or non-existence) of a certain reaction within the cell's network.

Fitness: a quantity measuring the cell's adaptation to its environment. The higher it is the more chance the cell has to reproduce.

Glycolysis: the metabolic pathway processing Glucose into pyruvate and energy (in the form of the net $2 \text{ ADP} \rightarrow \text{ATP}$ conversions).

Trunk of glycolysis: also known as the pay-off phase of glycolysis: the part of glycolysis that starts with G3P (Glyceraldehyde 3-phosphate) and end in pyruvate. It is called the pay-off phase as this is the part that produces ATP (while in the previous part an investment of ATP must be made).

Stoichiometric coefficient: the number of molecule of the given type participating in a reaction. In the reaction $2 \text{ H}_2 + \text{O}_2 \rightarrow 2 \text{ H}_2\text{O}$ the stoichiometric coefficient of H_2 is -2 , for O_2 it is -1 , and for H_2O it is 2 .

1 Introduction

All life on Earth is based on carbon, and it is hypothesized that if we ever find life elsewhere in the universe, it will also be carbon based. Carbon can bond with other carbon atoms and different atoms (especially hydrogen, oxygen and nitrogen) to build complex organic molecules. Cells use such complex organic molecules for a variety of functions such as constructing their membranes, enzymes and their whole structure using these molecules as building blocks. Cells therefore require organic and inorganic molecules that provide energy, and atoms necessary to synthesise these cellular building blocks.

The network of chemical reactions responsible for these processes is called the metabolic network (MN) of the cell. MN-s consist of multiple metabolic pathways, that perform certain function(s) that the organism requires. An example of a metabolic pathway is glycolysis that is the pathway processing glucose, a highly energetic organic compound into molecular building blocks such as pyruvate and energy, stored in the cell's currency metabolite ATP.

Considering the possibilities of chemistry it is easy to see that cells have infinitely many possible ways of metabolising their nutrients to the product they need, if we only impose the constraint that the individual atoms have to be conserved on both sides of reactions. Although different organisms utilize different chemical reactions in their MN-s, their core pathways are very similar among many different organisms. Certain pathways are conserved partially — eg. in glycolysis the Embden-Meyerhof-Parnas pathway [36] is used by most modern cells, some prokaryotes however use the Entner-Doudoroff pathway [11]. An other highly conserved pathway, the citric acid cycle (also known as the Krebs cycle) is used by all aerobic organisms¹. The reason for these similarities is not yet known, but most authors agree that it is a result of the evolution of the MN-s.

Biological evolution is a series of changes in the genetic material of organisms that is passed down to successive offsprings. The process of evolution uses simple facts: when organisms reproduce they don't always create perfect copies of themselves, resulting in a variation in the population they live in. This variation can cause different organisms to suit their environments better than others, and so those better suited will be able to reproduce more, passing on the genetic material responsible for the adaptations to the environment to their offsprings. The less suited organisms will reproduce less, and therefore eventually their genetic traits will disappear from the population. Biological evolution is responsible for the development of organisms from single-cells to multi-cell organisms as well as differentiation to plants and animals, and for the emergence of humans.

In this project we will examine whether the high degree of preservation of MN-s is an inherent feature of their evolution. To do so we will evolve populations of metabolic networks using an algorithm resembling biological evolution. We restrict the networks to simplified yet realistic subset of organic molecules and a toy model of chemistry. We will examine the reproducibility of evolution, i.e. whether the same MN-s and patterns of evolution emerge if the tape of life is played again.

¹Organisms that live in the presence of oxygen

In the rest of this chapter we will explain how MN-s can be modelled mathematically as graphs, and how biological evolution can be simulated on a computer, and why this project is of interest to a physicist.

In Chapter 2 we will show the methods used in the simulation with emphasis on the subset of molecules used, the calculation of the free energy change, the implementation of evolution in the code, the fitness-comparison of our organisms, and the data analysis.

In Chapter 3 we summarize the results of the project by show the results of the population simulations under different conditions.

In Chapter 4 we draw conclusions from the results of our simulations and consider them in the big picture of the mathematical understanding of biological evolution.

1.1 Metabolic networks as graphs

Thorough mathematical investigation of MN-s reveal fascinating topological properties, that make them similar to the social network of humans and the internet. These are small world character, scale-freeness, error-tolerance [21] and modularity.

A small-world network [37] is one in which the number of steps to connect any given pair of nodes — in our case chemical compounds — is small, and this number stays constant even as the network grows. In case of the human social networks this is colloquially known as the six degrees of separation [22]. A small-world character is desirable for a MN as it allows the network to withstand the loss of some of its nutrients. If a certain one is absent, an alternative pathway not much longer than the original can become active, producing the absent nutrient.

In a scale-free network the connectivity² is $P(n) = n^{-\gamma}$ for some constant γ , resulting in a few highly connected nodes (Hubs) and many scarcely connected nodes. This provides error-tolerance against random errors to the network, as unless a hub is removed, the performance (in our case the fitness of the MN) doesn't decrease significantly. It also makes the network different from a random graph [4], where every node is connected with a constant probability p , resulting in a Poisson distribution for the connectivity ($P(k) \approx \frac{\lambda^k e^{-\lambda}}{k!}$), as well as from a regular lattice, where every node is connected to a constant number of other nodes.

A module is "by definition, a discrete entity whose function is separable from those of other modules" [18]. Within a module, generally there are multiple possible pathways to achieve the same goal using so called precursor molecules. The module first converts its input to precursors, and then these are converted to the final product of the module. Usually the module also has the capability to transform precursors to other precursors, providing redundancy to the pathways. Precursors are useful, as if a module lacks one of its inputs, it is possible that through the conversion of other precursors it can still be functional, even if it functions at a reduced efficiency. Precursors also help evolution, and adaptation, as if the module can use one type of input and process it to precursors, a similar molecule can also be easily converted to the same precursor using perhaps a few additional reactions. For example if the cell is capable of processing glucose, using the

²The probability that a uniformly chosen node is connected to n other nodes

same enzymatic pathways it is also capable of processing 40 other similar molecules [1].

1.2 Evolution

Evolution works by exploiting the copying errors made in the genetic code of organisms when they reproduce. After such a reproduction the resulting offspring's performance might differ slightly from that of its predecessor at a certain task. In some cases this change is positive in the sense that it better equips the organism to suit its environment and allows it to multiply faster. In this case it and its consequent offsprings can outcompete the original organism and the unmutated ones. As Charles Darwin wrote "...Natural selection acts only by taking advantage of slight successive variations; she can never take a great and sudden leap, but must advance by short and sure, though slow steps." [7] It is difficult to imagine how highly sophisticated functions such as the eye, or feathers for flight, or even a complex metabolic network could have evolved using slight variations. [1] argues that complex structures have evolved non-adaptively as exaptations, as byproducts of evolution of other functions. [24] considers simple digital organisms that can obtain energy by performing logic functions. The organisms are provided an environment where they can reproduce (depending on the energy available to them) and mutate, and the more complex logical function they perform, the more energy they receive. They find that to get to the most complex logical operation (yielding the most amount of energy) many mutations are needed, and when appearing it often destroys other less complex logical operations. However once it is present, it provides such value that offsprings that don't have it are quickly eliminated by the competition.

Organisms need a way of passing down their genetic information to their offsprings. Most of them code their genetic material in the form of DNA. This uses a 4 letter alphabet of different base pairs to describe the genetic information necessary for the reproduction and functioning of the organism. When the organism multiplies this information must be duplicated and passed on to the offsprings. A typical bacterial genome consists of $\sim 10^6$ base pairs, and the human genome has 3.4×10^9 base pairs. Even though a multitude of error correcting mechanisms are in place [16], errors are made, for example *Escherichia coli* has an error rate³ of $10^{-9} - 10^{-11}$ [13]. These errors are most often point mutations that cause a small change in the genetic code of the organism.

The genome of our organisms consist of the list of reactions they are able to perform. This can be considered as a binary string of length 11790, the number of reactions in our 4 carbon network, with 0 for those reactions that do not appear, and 1 for those that do. In our model point mutations correspond to adding or removing a reaction from the MN of the cell.

Apart from random point mutations the genetic information of our cells can also change by the process of horizontal gene transfer. This is a method allowing Bacteria and Archaea to exchange genetic material between cells, and it is thought to be the main reason why bacteria can "learn" from each other eg. resistance to antibiotics [17][30]. We will examine how the presence of Horizontal Gene Transfer influences the evolutionary process.

³Errors per base pair

In real life cells use a variety of mechanisms to change the genetic information of cells such as gene duplication or gene insertion. We will not consider these in our model.

One of the largest problems in the mathematical modeling of biological evolution is the complexity of the fitness landscape. The fitness landscape is the function mapping the set of reactions in the metabolic network to a real number — the fitness of the MN. The true form of this function is not known therefore first toy landscapes were used to test phenomena, later simplified empirical landscapes were used. Recently the mapping of real fitness landscapes was started which confirm previous assumptions about the simplified models [8]. We will consider a realistic fitness landscape depending on the steady state of flux through our MN-s. The methods for calculating it are discussed in Section 2.4.

1.3 The chemistry of the problem???

When modelling metabolic networks one often has to make simplifications both in theoretical and computational research. These simplifications occur in defining the chemistry the cells can use, the objective function of cells, the environment the cells live in, as well as the anatomy of the cells themselves.

Modelling the intricacies of chemistry is a hopeless task with today’s computers, the fully quantum mechanical treatment of even a few thousand atoms is beyond the capabilities of supercomputers. To overcome this barrier artificial chemistries are often used, that simplify the rules, but grasp some important concept of chemistry. [9] describes some of these methods used. [19] use linear molecules consisting of 3 possible artificial atoms (called "1", "2", and "3" with the numbers showing how many bonds an atom can make with other atoms) to construct a metabolic network of organisms, and examine how they evolve. [15] considers "chemical reactions as graph rewriting operations, and uses a toy-version of quantum chemistry to derive thermodynamic parameters".

The thermodynamic constraints on evolution play an important role in the emergence of the MN-s currently used by organisms. [6] considers an exhaustive search of alternative metabolic networks to the trunk of glycolysis using a similar set of compounds and reactions used in this work. It finds that in environments similar to those found in a living cell (in terms of temperature and metabolite concentrations) the real glycolytic pathway outperforms every alternative, however if the physiological conditions are changed the real pathway can be outperformed.

Glycolysis is a highly conserved metabolic pathway that plays an important role in the metabolism of organisms in all three domains of life. It processes glucose into energy (in the form of ATP) and pyruvate, a simpler 3 carbon molecule. Glucose is an energy rich compound used by many organisms to store energy for a prolonged time, but it is also used as a source of carbon. Bacteria such as *E. coli* can use glucose as a source of carbon for the manufacture of the metabolites it needs for its growth (eg. amino acids and nucleotides). [23]

The glycolytic pathway can be divided into two parts: the preparatory phase and the payoff phase. In the preparatory phase glucose is split into two 3 carbon molecules: dihydroxyacetone phosphate (DHAP) and glyceraldehyde 3-phosphate (G3P) with the investment of 2 ATP. DHAP is then isomerized to an other G3P molecule, and G3P is

processed in the payoff phase. In this phase G3P is transformed into pyruvate yielding 2 ATP for both G3P molecules therefore giving a net yield of 2 ATP for every glucose processed. The pyruvate output of glycolysis is generally further processed, for example in aerobic organisms it is converted into CO_2 while releasing more energy in the citric acid cycle.

When organisms need to store energy they use the pathway of glycogenesis that creates glucose from simpler carbon molecules using many of the reactions of glycolysis in the opposite direction.

1.4 Evolution in the eyes of a physicist

Statistical physics makes very good predictions about systems where the number of particles is on the order of Avogadro's number, when these systems are in equilibrium or are closed. Living organisms are neither closed systems, nor are they in equilibrium. In order to maintain their non-equilibrium state they must obtain non-equilibrium materials — food or other nutrients — from their environment. If they fail to do so they reach equilibrium, or in other words die. [28] Therefore to consider living organisms we need the tools of non-equilibrium statistical physics.

Out of equilibrium systems are an actively researched area in statistical physics, and numerous concepts of it can be applied to biology.

One of the first people to quantitatively examine evolutionary processes R. A. Fisher wrote that [the theorem of natural selection] "bears some remarkable resemblances to the second law of thermodynamics." [14]. Both systems of statistical physics and evolving populations consist of a large number of particles (organisms) following relatively simple rules, based on probabilities. Due to the probabilistic nature of these systems exact solutions are very difficult to reach if even possible, and so one can only predict the large scale behaviour of the whole system. Stochastic methods originally developed in statistical physics play a crucial role in modelling the evolution of populations [3]. In this work we will use such a method, the Moran process [27] to simulate the evolution of populations, but another example for such model is the Wright-Fisher model [12].

Our model resembling biological evolution corresponds to a random walk in the space of available MN-s, that tries to optimize the fitness of our networks. The fitness landscape of even simple organisms such as ours is a very complicated function with many local minima and it is not known if the global optimum is accessible from every point in the space of all MN-s while transitioning through viable MN-s. [2] considered MN-s over a large set of chemical reactions and found that in all but the simplest cases the global optimum could be reached. Stochastic methods such as our model of evolution are successful in getting out of local minima, however can also be prone to oscillations around the global minimum

The process of biological evolution is an optimization process with inherently random elements. As such it is well suited to traverse a rugged fitness landscape in search of a global optimum, however unlike most stochastic optimization algorithms it can not easily traverse large obstacles in the fitness landscape. This is simply because if an organism becomes considerably less fit than its peers it will be quickly eliminated by the survival

of fittest phenomena.

Our work uses the well known formula to calculate the Gibbs free energy for our reactions in specific thermodynamic conditions. This formula uses the Gibbs free energy of reactions in standard conditions, which we got from experimental results where available, and estimated [6] where not. The fully quantum mechanical calculation of the free energy changes of reactions is feasible and could lead to more accurate answers using the same evolutionary methods described in this paper. Such a calculation of thousands of Gibbs free energies would be a job worthy of its own project, therefore we do not pursue it in this work.

2 Methods

2.1 Anatomy of the organisms simulated

A set of compounds and reactions (as used by [6]) was provided for the project by Bartłomiej Waclaw the project supervisor. This is the set of chemical compounds and reactions our organisms are allowed to use. The list of compounds consisted of 1966 CHOPN molecules of at most 4 carbon atoms, along with 13 so called internal metabolites. CHOPN molecules contain only carbon, hydrogen, oxygen, phosphor and nitrogen. Internal metabolites are compounds that are not CHOPN molecules fitting the previous criteria, but are essential cofactors to the reactions in the MN-s. The concentrations of the most important internal metabolites is listed in Table 3. In Table 1 we show an extract of the list of compounds.

Compound ID	Free energy of formation ΔG_0 (kJ/mol)	Chemical formula	Name	Charge
-7	-2292.39	ATP	—	-4
-6	-1424.91	ADP	—	-2
...				
-1	-155.758	H ₂ O	water	0
0	62.6568	CH ₃ -CH ₂ (OH)	ethanol	0
1	-247.929	CH ₂ -COOH	acetate	-1
2	23.8646	CH ₂ -CHO	acetaldehyde	0
3	-833.15	CH ₂ -CH ₂ p	—	-2
4	-1107.16	CH ₂ -COp	acetylphosphate	-2
5	10.21	CH ₂ -CO(NH ₂)	—	-2
...				

Table 1: Extract of the data file containing the compounds used

There are 11790 reactions of the at most 4 carbon compounds in the database used along with the ID of the compounds and the products and the free energy change of the reaction at the conditions described in [6]. An extract of the list of reactions is shown in

Table 2. The free energy changes are later calculated for arbitrary conditions as discussed in Section 2.2

Reaction ID	ΔG_0 (kJ/mol)	Compounds	Products
2	-28.3268	0,-7	3,-6
4	8.24999	1,-7	4,-6
5	-16.561	1,-7,-10	5,-6,-8
10	-7.83516	3,-1	0,-8
14	-41.6634	6	2,-1
18	-4.66344	6	38,-1
22	42.0077	7,-3	14,-4
25	257.103	7	50,-1
31	-25.83	8,-7	20,-6
...			

Table 2: Extract of the data file containing the reactions

Our program simulates the evolution of MN-s restricted to the metabolites and reactions provided. This is a realistic constraint as the trunk of the glycolytic pathway consists of such molecules.

In our model we assume that the direction of a reaction is determined only by its free energy change as defined under the physiological circumstances of the simulation. It is also assumed that given two reactions, both with free energy change larger (or smaller) than some pre-defined limit l the maximal flux through both reactions is the same. This is not necessarily the case in real cells. Apart from the free energy difference, the speed and direction of the reaction can be influenced by the free energy landscape between the initial and final states, also by the cell via the use of enzymes.

The anatomy of our cells is as follows: the cells have internal metabolites present inside their membranes with concentrations as shown in Table 3. The cells can import and export H_2O and CO_2 to and from their environments as these compounds can pass through the cell membrane. They can also import one predefined nutrient to process, and they can dispose one target molecule. Later this assumption will be relaxed, allowing the network to use multiple nutrients, and produce multiple products. The products of the network are only disposed of from the viewpoint of the metabolic pathway. They are often further processed by subsequent pathways, such as pyruvate in Section 1.3. The nutrient of the cell is available in excess in order to ensure that the fitness of the MN is limited by the reactions within the MN rather than the nutrient availability.

In certain simulations we allow the MN to dispose of phosphate (Pi), in real MN-s this could be used by other processes within the cell, such as the upper part of glycolysis. The network can also exchange the reduced form of Nicotinamide adenine dinucleotide (NADH) to its oxidized form NAD^+ . The oxidization of NADH occurs both in aerobic organisms (through oxidization via oxygen) and in anaerobic⁴ ones. In metabolic networks NAD^+ and NADH play an important role in redox reactions by carrying electrons between reactions. [23].

⁴Organisms that do not require oxygen. They can oxidize via alternative compounds, including iron and sulfate.

The success of a cell within a population is measured by its reproduction rate. If it reproduces often, it ensures its genetic material will be carried on by its offsprings. This means that if via a mutation a cell obtains a reproductive advantage, this advantage (ALLELE) can spread within the population due to the increased reproduction rate. Reproduction is a very energy demanding process, so we consider the fitness measured by the cell’s energy output. ATP acts as the energy currency in cells, and the ADP \rightarrow ATP conversion rate is considered to be proportional to the growth rate of the cells. We therefore use the flux through an auxiliary reaction⁵ performing this reaction. Later we consider more complex objective functions that reward biomass production, which is also a requirement for reproduction.

When organisms are considered as part of a population, the fitness of any individual depends on the fitness of others within the population. In a population where all but one cell has a fitness of 0.1 (on an arbitrary scale) and a single cell has fitness 0.5, this cell is obviously the fittest, and will reproduce more likely than the others. The same cell with fitness 0.5 in a population where the rest of cells have fitness 10, is much less likely to reproduce. Each of our cells has probability to reproduce, that is proportional to their current fitness value, normalized with the cumulative fitness of the population. We do not consider cells with negative fitness, considered unviable for reproduction. At each reproductive step in the algorithm the cell to reproduce is drawn from a probability density function that is proportional to the fitness of each cell (up to normalization), using the Moran process described in Section 2.3.

We consider the size of the population to be constant, fixed by the carrying capacity of the environment. This means that every time a cell reproduces, a cell must die to accommodate the newborn one. The deceasing cell is chosen uniformly from the population, therefore giving the expected lifetime of a cell to be 1 generation.

The cells in a population are considered to be close to each other, so any two cells can meet and exchange genetic information in the process of horizontal gene transfer.

2.2 Calculating the free energy change

The Gibbs Free Energy is the amount of energy at a given reaction that can be used to do work, or if it is negative, then the amount of work that has to be done on the system for the reaction to happen.

The list of reactions provided the project supervisor contained the following for each reaction: the list of compounds the reaction uses, the list of products the reaction produces and the free energy change of the reaction (experimentally when known, otherwise estimated). This list is similar to that used by [6].

The free energy changes provided were at the conditions $T = 25^\circ C$ pH= 7.0 $I = 0.2M$ (ionic strength) and all metabolite concentrations set to 1 M calculated by [6].

Assuming a reaction of the form $n_1A + n_2B \rightleftharpoons n_3C + n_4D$ where the concentration of substrate A is denoted by $[A]$, and similarly for the other substrates, n_1 denotes the number of molecules of type A that take part in the reaction and ΔG^0 the free energy

⁵Defined in Section 2.4

Temperature	293 K
[ATP]	$10^{-1}M$
[ADP]	$10^{-2}M$
[AMP]	$10^{-4}M$
[NAD ⁺]	$10^{-1}M$
[NADH]	$10^{-4}M$
[Pi]	$10^{-3}M$
[PPi]	$10^{-3}M$
[CO ₂]	$10^{-5}M$
[NH ₃]	$10^{-5}M$

Table 3: The environmental variables considered

change of this reaction at standard conditions. The change in free energy for arbitrary T and concentrations is given by:

$$\Delta G = \Delta G^0 + RT \ln \frac{[C]^{n_3}[D]^{n_4}}{[A]^{n_1}[B]^{n_2}} \quad (1)$$

At the beginning of the program the reactions are read in from a file, and the free energy changes are re-calculated for the specified conditions as in Table 3. The internal metabolites that are not shown in the table do not appear in the reactions used by our MN-s. Their concentrations have been set to 1.

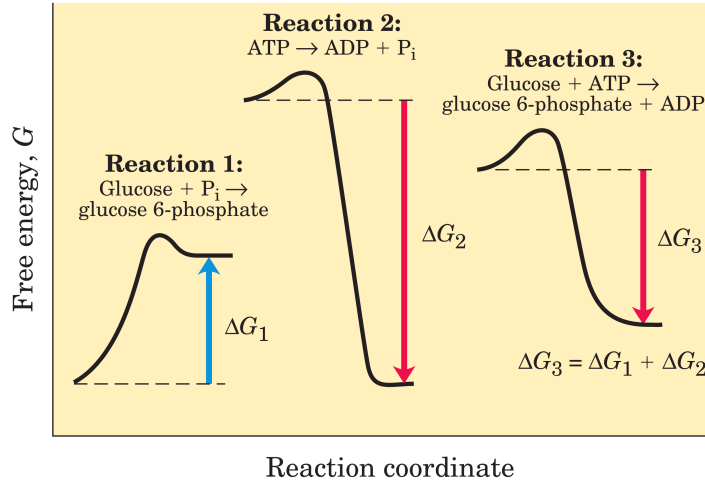


Figure 1: Free Energy landscapes of three reactions, showing the different flux-constraints imposed in our model. Figure reproduced from [23]

The constraints imposed on the flux of each reaction, depending on the free energy change of them are as follows: for the m th reaction the flux v_m has to satisfy $0 \leq v_m \leq 1$ if $\Delta G \leq -L$ eV, $-1 \leq v_m \leq 0$ if $\Delta G \geq L$ eV. As in the real world the reactions happening in a cell are usually reversible. An example for this is the reaction of carbonic acid and water $\text{H}_2\text{CO}_{3(l)} + \text{H}_2\text{O}_{(l)} \rightleftharpoons \text{HCO}_3^-(\text{aq}) + \text{H}_3\text{O}^+(\text{aq})$. We allow reactions with free energy change between a constant $-L$ and L eV to happen in any direction. Currently the value

of $L = 10$ eV but it is a parameter easily changed in the program. In Figure 1 we show possible cases of this. Assuming $\Delta G_1 > L$ Reaction 1 would have its flux restricted as $-1 \leq v_1 \leq 0$, also if $\Delta G_2 < -L$ v_2 is restricted as $0 \leq v_2 \leq 1$, and if $|\Delta G_3| \leq L$ we have $-0.5 \leq v_3 \leq 0.5$.

In real life the likelihood of these reactions happening, and so the flux through them depends on the height of the potential barrier between the original substrates and the end products. If the barrier is high the reaction might not happen unless the amount of energy required to overcome it is invested. Cells are able to lower the heights of such barriers using catalytic enzymes, therefore our model is not unrealistic by neglecting their role in determining the directions and fluxes of the reactions.

2.3 In silico Evolution

To simulate biological evolution on a computer we need three things: replication, mutation and competition. The sophisticated interplay of random mutations and the more deterministic selection gives rise to the success of evolution. The basics of these concepts can easily be implemented in our program, giving a process similar to biological evolution. Our simulations always start with a homogeneous population, all cells are identical. The population later diverges as a result of random mutations. The real evolution of the genomes of organisms uses a variety of methods some of which are discussed in Section 1.2. Of these, our cells use point mutations and later horizontal gene transfer.

Point mutations either add or delete a reaction to the MN. Simply adding a reaction to those available to the cell at random from the list of all the reactions is unlikely to result in a reaction that could be used by the cell. This is because with a high probability the added reaction would be disconnected from the current MN. As discussed in Section 2.4 the flux through these reactions would be zero. Therefore when adding reactions, we only consider those that are linked to one of the current reactions, either by using a compound that the network is capable of producing, or providing one that it can consume. This way the graph of the reactions and compounds available to the cell stays a connected graph (disregarding deletions). Choosing the list of reactions that can be added uses the neighbour-list defined in OUR ALGORITHM APPENDIX X. When deleting a reaction every currently available reaction has equal probability of being deleted. This can and does result in disconnected graphs, but such disconnected parts are usually small, otherwise they bear too high a cost to maintain and are therefore an evolutionary disadvantage.

The most elementary event in a population of our organisms is the reproduction of a cell, implemented using the Moran process [27]

At every step of the Moran process a single member of the population is chosen to reproduce (with or without mutations) and an other member of the population dies, to keep the size of the population constant. At every such step the cell has some probability of mutating, both for a point mutation (p_{point}), and for horizontal gene transferring a reaction (P_{HGT}) from an other randomly chosen cell. This process is a random walk in the space of all possible genes or MN-s allowed by the chemistry of the cells. This walk is then mapped to the fitness landscape using the objective function of the cells.

There are two contributions to the fitness measure of a cell, its energy production, and the number of reactions in its MN. The first objective function we used awarded a fitness score of 1 for every $\text{ADP} \rightarrow \text{ATP}$ executed by the cell. For every reaction in the MN, the cell pays a small cost k_{reac} from the fitness score. This is because cells usually control their reactions through the use of enzymes that they have to manufacture, and code in their genetic code. Should we not include this cost the cell’s MN-s could grow without bounds until every reaction in our list would appear within them. This could then be considered a best network. Later we consider more complex objective functions that reward biomass production, at different weights compared to the energy production.

The probability density function (PDF) of which cell is selected for reproduction is proportional to the fitness of each cell (with the caveat that cells with negative fitness are deemed unviable and are not allowed to reproduce). To know this PDF it is necessary to know the fitness of each cell at any given time point (for the normalization), and therefore it would be impractical to use this to choose the cell that will reproduce. Instead we sample as follows:

1. We uniformly chose a cell in our population — c_i
2. We generate a random number from the distribution $U(r, M)$ where M is the maximal fitness value a cell can take
3. If the fitness of c_i , $F_{c_i} \geq r$ we accept the change, if not we start the process again

This process can be shown to result in a sampling of cells equivalent to that of the PDF proportional to the fitness of each cell.

2.4 Flux Balance analysis

To calculate the throughput of the metabolic network of our organisms we use flux balance analysis [29].

The goal of flux balance analysis is to calculate the steady state fluxes (\mathbf{v}) through all the reactions, subject to some constraints, while maximizing a linear function $Z = \mathbf{c}^T \mathbf{v}$ of the fluxes called objective function, in the solution space allowed by the constraints.

When using flux balance analysis we represent the MN as a stoichiometric matrix S ($m \times n$), with each row corresponding to a compound in the network (n compounds), and each column corresponding to a reaction (m reactions). In each column we have the stoichiometric coefficients of the given reaction that correspond to the compound of the given row. Negative stoichiometric coefficients are used for the metabolites consumed, positive for those produced, and zeros for the metabolites that do not participate in the given reaction.

We want to find a set of steady state fluxes $\mathbf{v} = (v_1, v_2, \dots, v_m)$ that obey the principle of mass conservations. If we represent the concentrations of our compounds by $\mathbf{x} = (x_1, \dots, x_n)$ this condition is expressed as $\frac{d\mathbf{x}}{dt} = 0$, no compound is depleted or accrued, the rate a metabolite is consumed must equal the rate it is produced. Using the

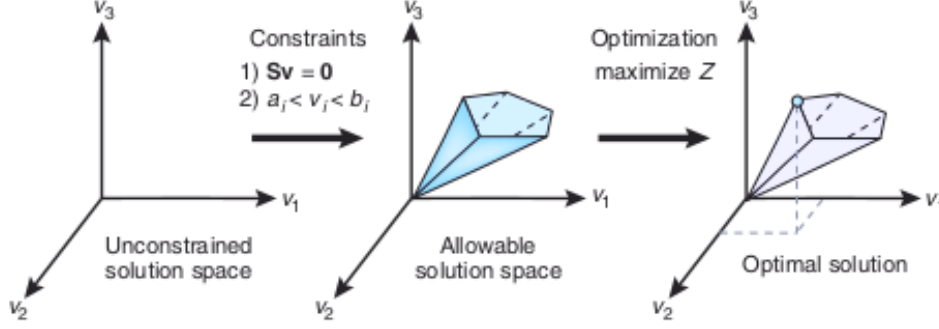


Figure 2: The process of flux balance analysis. First we apply the steady state constraints along with further constraints on the fluxes, then we maximize the objective function in the allowable solution space found. Figure reproduced from [29]

stoichiometric matrix the steady state condition can be expressed as $\frac{dx}{dt} = S\mathbf{v} = \mathbf{0}$ (the allowable solution space in Figure 2). These equations take the form

$$\begin{aligned}
 S_{1,1}v_1 + S_{1,2}v_2 + \dots + S_{1,m}v_m &= 0 \\
 S_{2,1}v_1 + S_{2,2}v_2 + \dots + S_{2,m}v_m &= 0 \\
 &\dots \\
 S_{n,1}v_1 + S_{n,2}v_2 + \dots + S_{n,m}v_m &= 0
 \end{aligned} \tag{2}$$

The network must however exchange some special compounds with its environment such as the nutrients and the end-products of the MN. For example the nutrients of our network on Figure 3 is $\text{CO}=\text{CH}-\text{CH}(\text{OH})-\text{COp}$ and water, while its end products are lactate and CO_2 . Incorporating the exchange of certain compounds with the environment of the MN could be done through relaxing the constraint that the equation corresponding to the given compound among those in Equation 2 have to equal zero. This introduces complications, as often the amount of these compounds produced appears in the objective function $Z = \mathbf{c}^T \mathbf{v}$. To overcome this we introduce auxiliary reactions to the stoichiometric matrix S , for the compounds the cell consumes and produces. Such an auxiliary reaction is for example $\rightarrow \text{H}_2\text{O}$, that "creates water out of nothing", or in other words corresponds to the potential water intake of the cell.

We want to maximize the objective function $Z(\mathbf{v})$ in the allowable solution space. The form of the objective function is $Z = \mathbf{c}^T \mathbf{v}$ with the elements of \mathbf{c} being the weights of the fluxes through each reaction in the objective function. In the simplest cases $c_i = 0$ for all but a single value of i , in which case the goal is to maximize the flux through a single reaction, which in the literature is often chosen to be the biomass removing auxiliary equation[29]. In our case the original objective function used is the one converting ATP to ADP. This reaction occurs in cells, $(\text{ATP} + \text{H}_2\text{O} \rightarrow \text{ADP} + \text{P}_i)$, and it releases energy. As cells store energy in ATP molecules, by maximizing the flux through the ATP producing reaction, we are maximizing the energy output of the cell. In many cases this is synonymous with maximizing the growth rate of the cell. The auxiliary reaction corresponding to the $\text{ATP} \rightarrow \text{ADP}$ conversion does not contain the release of phosphate in this test network. This is because the nutrient of the network contains phosphate while

the end product does not. In such cases the phosphate produced by the ATP hydrolysis would have to be removed by an other auxiliary reaction. To make the program a bit more efficient we do not consider this additional reaction now, however in later simulations we will.

There are many software packages capable of solving linear programming problems, we use the Gnu Linear Programming Kit (GLPK) [25]. GLPK is implemented in C, and has all the functionality we need to calculate the fitness of our metabolic network. For the code calculating the fitnesses see the function `calcThroughput` in APPENDIX X.

Flux balance analysis can be used to incorporate a wide range of other concepts, such as non-linear objective functions, regulatory and energy balance analysis constraints[31]. Our choice of implementation limits us to use only linear objective functions; this issue is addressed in Section 4.

Example of flux balance analysis

Here we give an example of how flux balance analysis is used to calculate the fitness of a MN. We consider a toy network, that has an easily verifiable solution. The network is shown on Figure 3, it is a simple network that was used to test the part of the program calculating the optimal fluxes.. For the purpose of this example let us consider the cost of a reaction is $k_{reac} = 0.01$.

The metabolites of the network (in green) have been denoted by letters A, B and D for brevity. The stoichiometric matrix of this metabolic network is shown at Equation 3 (below), with the metabolites the rows correspond to are shown on the left of the matrix. The first three columns of the matrix correspond to reactions 5151, 5133 and 131 respectively. The other columns correspond to auxiliary reactions, providing the nutrient of the network (A), removing the end-product (lactate), providing water, providing CO₂, and converting ATP to ADP in this order. Auxiliary reactions are not shown on figure of the MN-s.

$$\begin{array}{l} \text{A} \\ \text{B} \\ \text{D} \\ \text{lactate} \\ \text{water} \\ \text{CO}_2 \\ \text{ATP} \\ \text{ADP} \end{array}, S = \begin{pmatrix} -1 & 0 & 0 & +1 & 0 & 0 & 0 & 0 \\ +1 & -1 & 0 & 0 & 0 & 0 & 0 & 0 \\ 0 & +1 & -1 & 0 & 0 & 0 & 0 & 0 \\ 0 & 0 & +1 & 0 & -1 & 0 & 0 & 0 \\ -1 & -1 & 0 & 0 & 0 & +1 & 0 & 0 \\ +1 & +1 & 0 & 0 & 0 & 0 & -1 & 0 \\ 0 & +1 & 0 & 0 & 0 & 0 & 0 & -1 \\ 0 & -1 & 0 & 0 & 0 & 0 & 0 & +1 \end{pmatrix} \quad (3)$$

The linear equations that are implied by $S\mathbf{v} = \mathbf{0}$ for the example network of Figure 3 are shown below, at Equation 4. Constraints on the system are imposed in two ways. Firstly by $S\mathbf{v} = 0$ we require that the fluxes represent the steady state solution, and secondly by restricting the values of v_i by inequalities ($v_{lower,i} \leq v_i \leq v_{higher,i}$) we can restrict the flux of individual reactions, their directions, and the amount of compounds the cell can take up and dispose of.

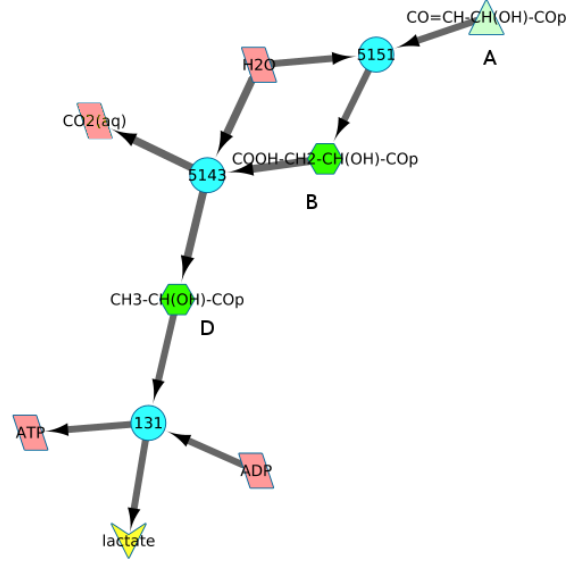


Figure 3: Example of a simple network. Reactions: light blue, metabolites: green, nutrient: light green, end-product: yellow, internal metabolites:red

$$\begin{array}{ll}
 \text{A} & -v_1 + v_4 = 0 \\
 \text{B} & v_1 - v_2 = 0 \\
 \text{D} & v_2 - v_3 = 0 \\
 \text{lactate} & v_3 - v_5 = 0 \\
 \text{water} & -v_1 - v_2 + v_6 = 0 \\
 \text{CO}_2 & v_1 + v_2 - v_7 = 0 \\
 \text{ATP} & v_2 - v_8 = 0 \\
 \text{ADP} & -v_2 + v_8 = 0
 \end{array} \tag{4}$$

The bounds on the given reactions are as follows:

$$\begin{array}{l}
 0 \leq v_1 \leq 1 \\
 0 \leq v_2 \leq 1 \\
 0 \leq v_3 \leq 1 \\
 0 \leq v_4 \leq 10 \\
 0 \leq v_5 \leq \infty \\
 0 \leq v_6 \leq 40 \\
 0 \leq v_7 \leq 40 \\
 0 \leq v_8 \leq \infty
 \end{array} \tag{5}$$

The limiting fluxes should in any case be those of the real reactions (in our case v_1, v_2 , and v_3). The cell's nutrient intake (v_4) is set to a high but finite value, this is important as a this puts a high bound on the fitness function. Such a theoretical upper bound for the fitness function must be known, as it is used in the algorithm when we select the next cell that reproduces. The cell's water intake and CO_2 disposal are limited by a high value for the same reason. Care is taken in order to keep these values high enough not to be

limiting for the evolution of the network. The pyruvate removal and the $\text{ATP} \rightarrow \text{ADP}$ conversion reactions need not be bounded, as they are limited by the nutrient uptake of the cell.

The weights of the objective function in this case are $c_8 = 1$ and $c_i = 0$ for $i \neq 8$, giving the value of the objective function to be $Z = v_8$, the energy output of the cell. This is to be maximized within the constraints.

The optimal solution of the equations with the bounds given at Equation 5 is

$$v_1 = 1, v_2 = 1, v_3 = 1, v_4 = 1, v_5 = 1, v_6 = 2, v_7 = 2, v_8 = 1 \quad (6)$$

Giving the value of the objective function to be $Z = v_8 = 1$. As the MN has 3 reactions the final fitness value for it would be $Z - 3 \times k_{\text{reac}} = 1 - 3 \times 0.01 = 0.97$

2.5 Data analysis

To visualize the resulting MN-s we use the open source biological network visualization tool Cytoscape [32]. Figures showing metabolic networks in this work have been generated using this software (eg. Figure 3). Our program was equipped with the functionality to export MN-s into the XGMML format that Cytoscape can read.

While MN-s can be visually compared using Cytoscape, doing so for more than a handful of networks is a cumbersome task, therefore we considered some summary statistics to compare MN-s resulting from our simulations.

While the simulation is running, approximately every 10000 mutations some key descriptors of the populations are written out to a log file. This allows us to monitor the progress of the populations while the simulation is running, and also to plot the timeline of their evolution. Examples of such graphs can be found in Section 3 (eg. Figure 5). The descriptors calculated are: the fitness of the fittest network in the population, the average fitness of the population, the entropy of the population, the number of reactions in the fittest network, the average number of reactions in the population, the number of used reactions⁶ in the best MN, and the average number of such reactions per MN in the population.

Entropy is used as one of the measures of the diversity of the population. It is calculated as: $S = -\sum_{i=1}^M n_i \log n_i$ where n_i denotes the number of cells of type i , and the sum runs through all the different types of cells in the population. This entropy measure is linearly proportional to $S_{\text{statphys}} = \sum_i p_i \log p_i$, with p_i being the probability of a given state, used in statistical physics. As we are considering a population with $N = 100$ cells, the minimal entropy is $S_{\text{min}} = -100 \log 100 = -460.52$, this value is attained when every cell in the population is identical ($p_{i_1} = 100$, and $p_i = 0$ for other i values), as is the case initially in our populations. its maximal value is $S_{\text{max}} = 0$ attained when every cell is different in the population. This happens when the mutation rate is very high (eg. $p_{\text{point}} = 1$).

To compare networks between populations we define a similarity index $M_{i,j}$ between two MN-s i and j , calculated as follows: we count the reactions appearing in both MN-s, then

⁶Reactions with non-zero flux in the optimal solution to the flux balance analysis problem

divide this count by the number of reactions in the larger of the two networks. This means $0 \leq M_{i,j} \leq 1$, with these extreme values attained if the two MN-s share no reactions, and if they are identical, respectively. We calculate two similarity indices for each pair of MN-s, one for every reaction in the two MN-s ($M_{i,j,all}$) and one only for those reactions that have non-zero flux through them in the optimal solution ($M_{i,j,used}$). This is an important distinction, as for a high mutation rate, and small k_{reac} value the two MN-s might have a lot of unused reactions that differ amongst them, but their used reactions could be the same. As the indices are symmetric ($M_{i,j,all} = M_{j,i,all}$ and $M_{i,j,used} = M_{j,i,used}$) instead of two separate plots, we plot

$$M_{i,j} = \begin{cases} M_{i,j,all} & i \leq j \\ M_{i,j,used} & \text{otherwise} \end{cases}$$

Thus we show the similarity indices calculated using all reactions above the diagonal of the plot, and those calculated using the used reactions below the diagonal. The diagonal entries are always 1-s as any network is equivalent to itself. We plot the two regions separately to make distinguishing between the two parts easy.

While the simulations are running, we save the states of the populations at 10 occasions, both to be used as checkpoints if the calculation doesn't finish, and also to be able to look at how the networks evolved. At these checkpoints the MN of every cell in the population are written out (in the **XGML** format). This allows both the visualization of the networks and also their comparison using the similarity indices between them. As plotting the similarity indices as a matrix (as on Figure 10) for every population at every checkpoint would be impractical, we instead consider the similarity indices of MN-s within a population compared to the fittest network in the population, resulting in a vector of $N - 1$ similarity indices (we don't compare the fittest network with itself). This would correspond to the first column (or row) of each population on the similarity matrix plot, for example Figure 10.

These similarity indices are then summarized using their Inverse Participation Ratio. The similarity indices of each population are divided into 10 bins, and the IPR of the proportion of elements in the bin are calculated, using $IPR = \sum_{i=1}^{10} \frac{1}{p_i^2}$ where p_i is the proportion of similarity indices in bin i (this ensures normalization, $\sum_{i=1}^{10} p_i = 1$). The minimum of this IPR value is 1, attained for a completely homogeneous population, while the maximum of 10 is attained when each of the 10 bins have an equal amount of similarity indices within them (the most disordered state). At each checkpoint the IPR of the two similarity indices $M_{i,j,all}$ and $M_{i,j,used}$ are calculated along with the IPR of the fitness values at the checkpoint.

2.6 Technical remarks

Whenever we add a reaction to a MN we have to find the reactions that connect to the current network, through at least one shared metabolite, as described in Section 2.3. It is very time consuming to list all metabolites currently in the network, then search through all the reactions to see if any of the used metabolites are used within them. To speed up the process of selection, at the beginning of the program a neighbour-list is generated that

contains for every reaction a list of neighbouring reactions, that share at least 1 compound with it, excluding internal metabolites. For example in our example network on Figure 3 reactions 131 and 5143 are neighbouring, as they share the metabolite $\text{CH}_3\text{-CH(OH)-COP}$, but reactions 131 and 5151 are not neighbouring. Using this neighbour-list our program can now rapidly find the possible reactions to add to a network.

An important component of a Monte Carlo simulation is the source of pseudorandom numbers. In our program we use the Mersenne Twister [26] generator, provided by the Boost C++ libraries [33]. This generator is fast, provides high-quality pseudorandom numbers and has a period of $2^{19937} - 1$, and will therefore provide more than enough pseudorandom numbers for our simulations.

To speed up calculations we performed multiple parallel simulations of populations on different computers. In order for every population to be different, we used different initial values to seed the pseudorandom number generator. For the sake of reproducibility these seeds are noted with the output of the simulations.

In a population usually there are multiple "copies" of any given cell, as the rate of mutations is low, eg. for $p_{point} = 0.1$ only every tenth reproduction results in a new type of cell. To make our program more efficient we consider the population as a list of cell types $\{t_i\}$ $i = 1 \dots N$, and a list of cells $\{c_j\}$ $j = 1 \dots N$. The cells store integers referencing to the given type, $c_5 = 2, c_2 = 1$ means that the fifth cell is of type 2, and the second one is type 1. If cell 5 dies and cell 2 is chosen to reproduce without mutation, this can be expressed as $c_5 \leftarrow c_2$ making $c_5 = c_2 = 1$. The most time consuming operation in our program is solving the linear programming problem that needs to be calculated whenever a new cell is created. By using this index-based population we have no need to do solve it when reproduction happens without mutation. For lower mutation rates such as $p_{point} = 0.01$ this means a significant performance increase.

3 Results

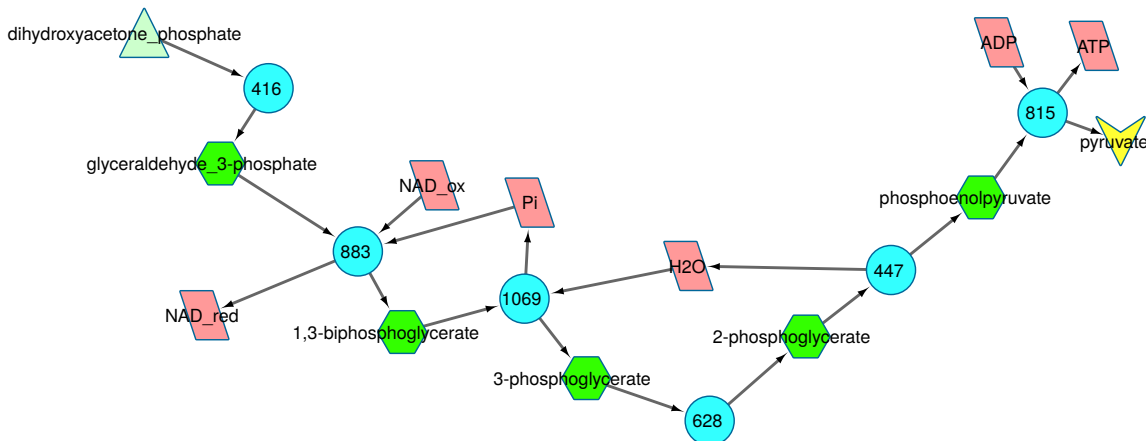


Figure 4: Trunk of the glycolytic pathway with the additional reaction at the beginning

The first simulation we run used a modified version of the trunk of glycolysis as a starting network. This modified network starts from DHAP, one of the products of the upper part of glycolysis, and ends in pyruvate. The starting network is shown on Figure 4. Reaction 416 was added to the usual lower glycolytic pathway at the beginning of the MN. This reaction transforms DHAP into G3P the compound normally considered the first metabolite of lower glycolysis. Apart from this the ATP producing reaction 633 was removed, in exchange for 1069, that fulfills a similar role to 663, but instead of creating ATP from ADP it discards the phosphate group it sheds from 1,3 biphosphoglycerate.

The fitness cost of having a reaction within the MN was set to $k_{reac} = 0.001$ with the rate of point mutations as $p_{point} = 1$ in order to have as much change and improvements as possible. The fitness function used here was the flux of ADP to ATP conversion minus k_{reac} times the number of reactions in the MN.

The initial ATP flux of this network is 0.5, with the limiting reaction being 883, that has a free energy change of 1.71 eV at the conditions given by Table 3. This is a good initial network as it has plenty of potential to improve, eg. by "rediscovering" reaction 633, or finding completely new paths from the nutrient of the MN to the end product. For the sake of brevity we shall refer to this simulation as Simulation 1.

When running the simulations, we started with 20 identical, uniform populations with 100 cells in each, and provided a different seed for the pseudorandom-number generators used, therefore the populations evolved independently from one another. Not all the 20 populations finished the simulation due to technical difficulties. Of those that did, we show diagnostic plots for 3 typical populations that showed some improvement during the simulation.

The fitness of the best network within 3 typical populations of Simulation 1 and the average fitness of those populations are shown as a function of the number of generations since the initial network on the first two graphs of Figure 5. We normally save the summary statistics approximately every 10000 mutations, in this case 100 generations, but keep the values of these summary statistics for the intermittent generations in-memory. If there was a significant improvement in the fitness of the population we write the intermittent steps out too, so the transition of the population can be observed.

An extract of such intermittent steps is shown on Figure 6 from Simulation 2, that has a lower mutation rate than Simulation 1. The number of generations it takes for a cell with relative fitness advantage s to take over a population is calculated as $T \approx \frac{s+2}{s} \ln N$ [35]. This is called the expected time of fixation. In the population shown on Figure 6 the original population has a fitness of 0.48 and the fitness of the mutant is 0.98, therefore the fitness advantage is $s \approx 2$, giving us the time for fixation as $T \approx \frac{2+2}{2} \ln 100 \approx 9.21$ generations. This coincides with the observed time of fixation, the time it takes for the average fitness of the population to "catch up" with the fitness of the best cell. We plot a population from Simulation 2 rather than Simulation 1, as the calculation of the aforementioned formula uses the assumption that mutations are rare. This assumption is better satisfied in Simulation 2 where the expected number of mutations per generation is 1, as opposed to 100 in Simulation 1.

As such fixations remain invisible on a plot whose x axis is on the order of $10^5 - 10^6$ such as Figure 5, the first and second pair of graphs are very similar. In consequent diagrams

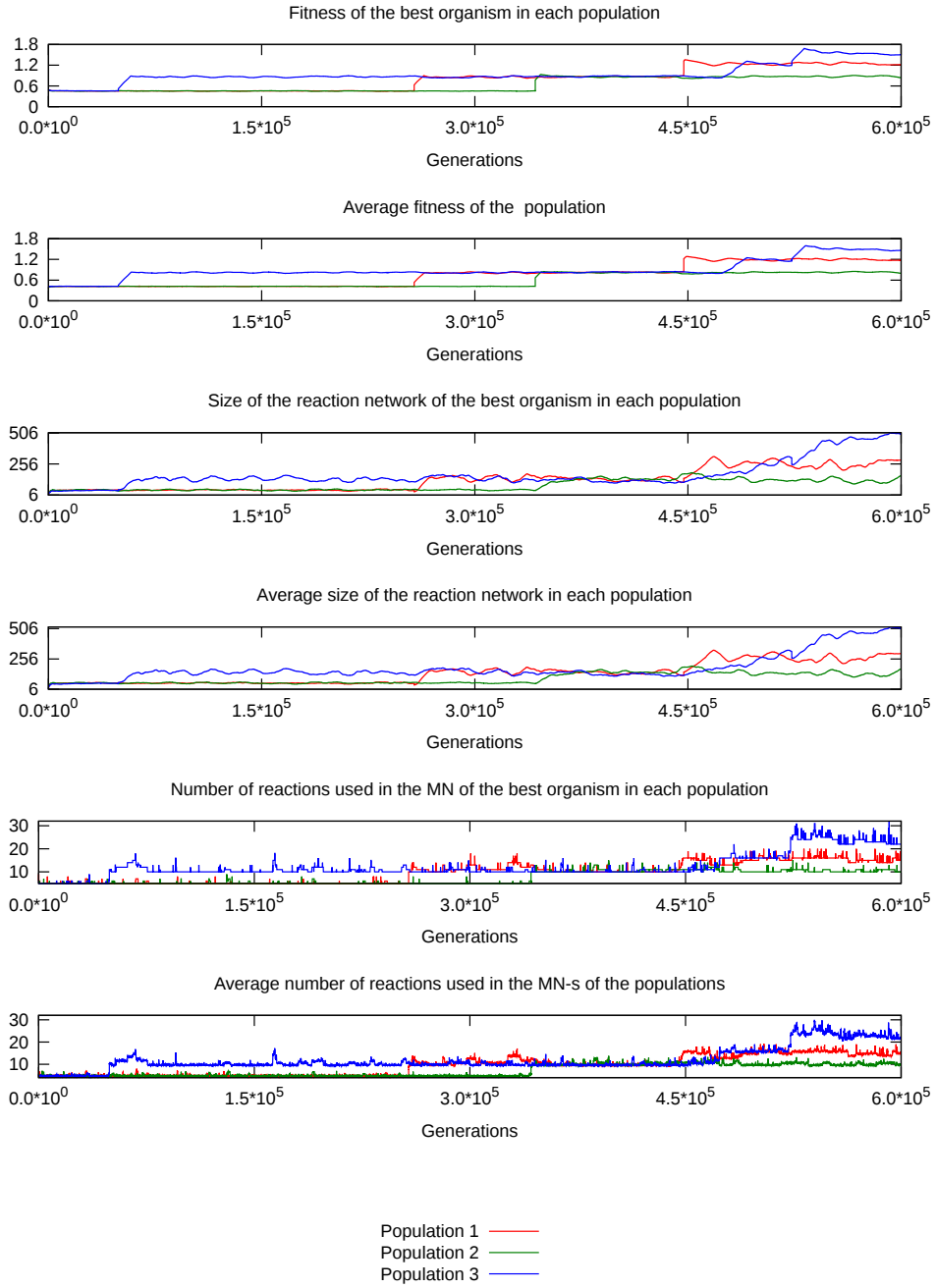


Figure 5: Diagnostic plots for 3 typical populations of Simulation 1

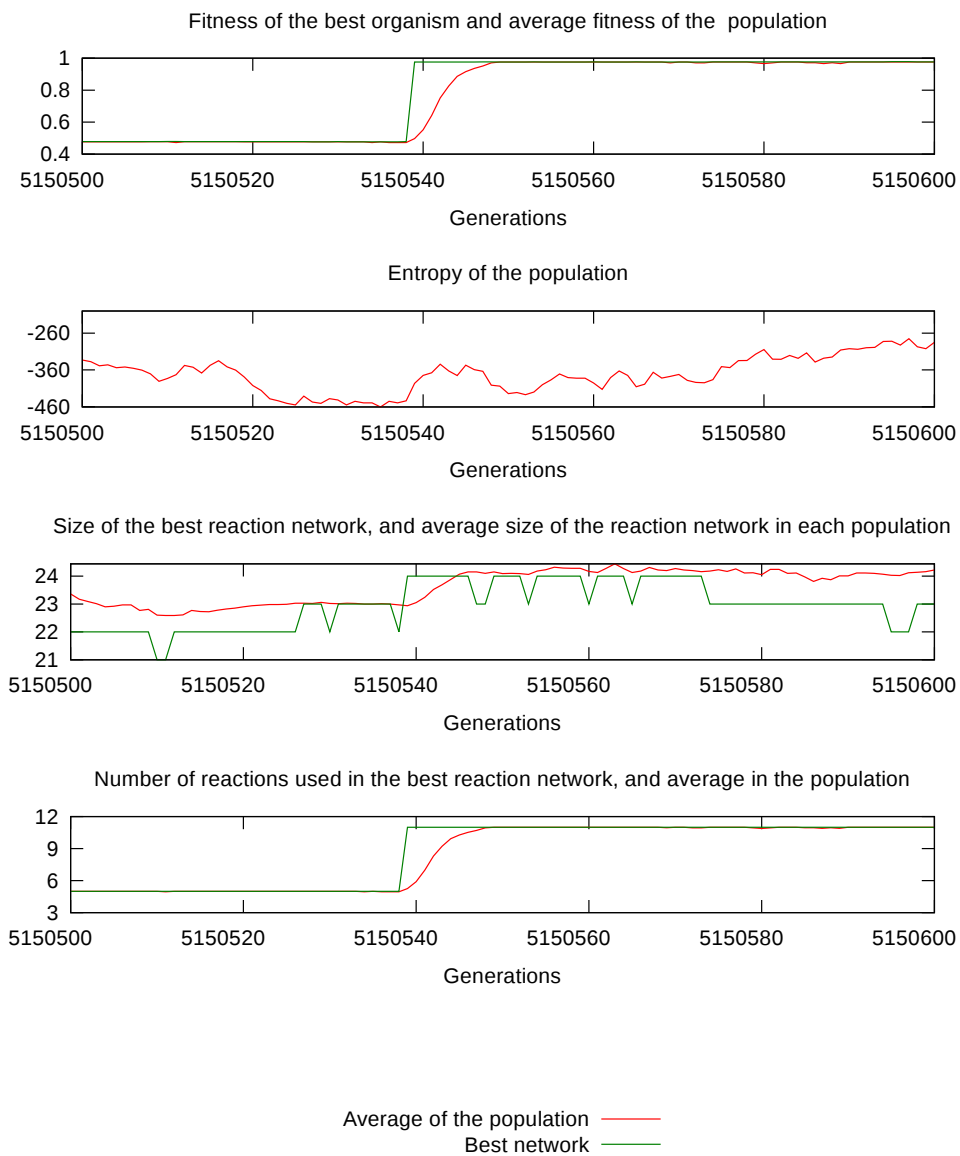


Figure 6: Extract of summary statistics of Population 1 of Simulation 2 showing the fixation of a beneficial mutation

we shall show only the graphs for the average of the population (average of fitness, total number of reactions, and number of used reactions).

All populations in Simulation 1 have improved their fitness by increasing the ADP ATP conversion rate by at least 0.5 some of them by 1. The magnitudes of any single improvement was 0.5 — this means every pathway uses at least one reaction that is considered to be bidirectional in our model. The times of improvements are distributed approximately uniformly and after any jump-improvement in all curves we can observe a slight decline in fitness. This phenomena is due to the MN-s obtaining more and more reactions of which few are only used, as can be seen on graphs 3 and 4 of Figure 5. Observe that the number of reactions in the MN-s start to increase when the fitness does. The number of used reactions are shown on the last pair of graphs on Figure 5, for the best network and for the average network. The reaction network with ATP production of 0.5 uses ~ 6 reactions, to produce 1 ATP the network needs ~ 10 , and for 1.5 ATP it needs 14.

The used reactions of the best performing network of Population 3 of Simulation 1 are shown on Figure 7. The network found alternative pathways to bypass the restrictions imposed by the bounds on the reaction fluxes. The two longer alternative pathways (to the right) meet at phosphoenolpyruvate, and there they diverge again, one converting an previously produced AMP (adenosin monophosphate) to ATP while the other converting ADP to ATP. We observe similar meeting and diverging paths in the simulations that follow. The reactions of the real glycolytic network are shown in yellow on this figure. In real glycolysis 3-phosphoglycerate is isomerized to 2-phosphoglycerate, this network therefore performs almost all reactions that real glycolysis does, but not in a single path.

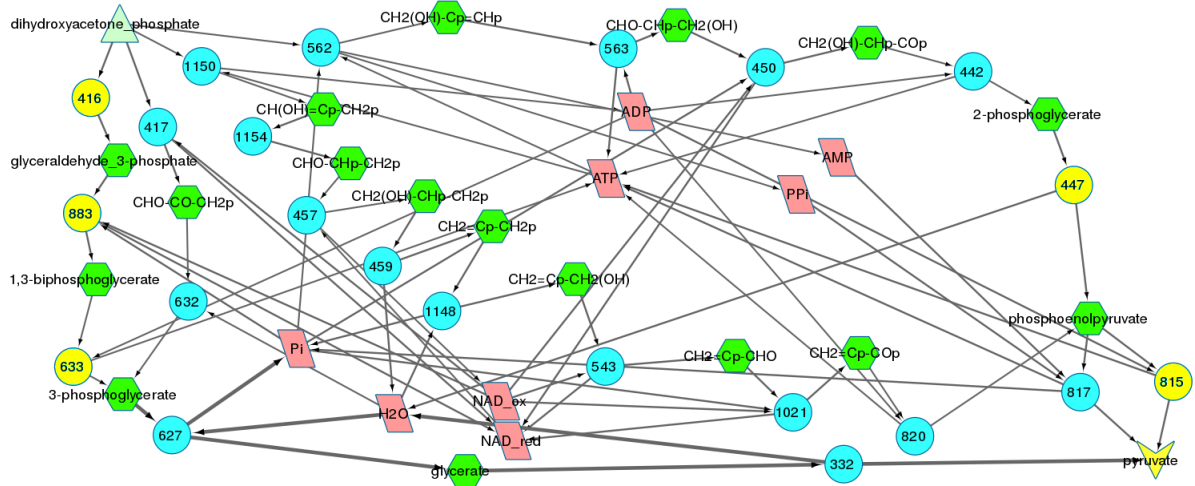


Figure 7: Reactions with nonzero flux in the fittest network at the end of the Simulation 1 in Population 3. The reactions of real glycolysis have been coloured yellow. Thin arrows mean a $v = 0.5$, thick ones mean $v = 1$.

An overview of the MN-s is shown on Figure 8 at three points in time, the beginning of the simulation (left), at the midpoint, after 1.5×10^5 generations, and the final stage. The disconnected nodes at the bottom of the left plot are yet unused internal metabolites. Note the small disconnected components of the middle and the left plots. These are a result of the mutation method implemented in our program, described in Section 2.3.

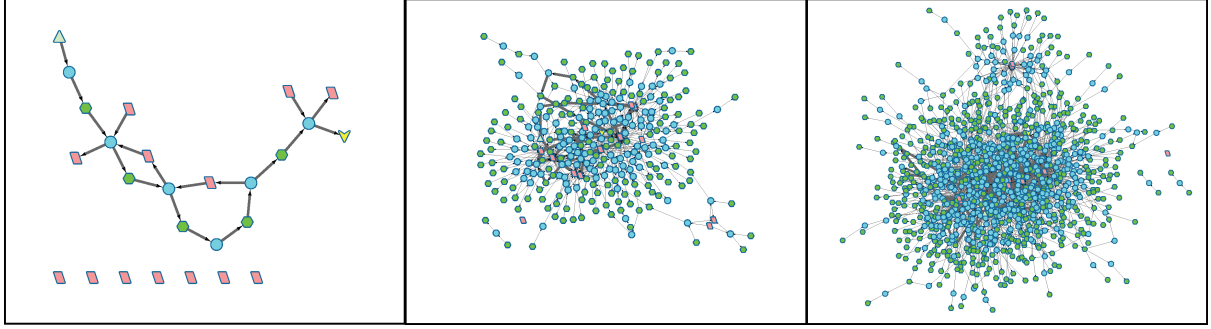


Figure 8: Overview of the best performing metabolic network of Population 3 of Simulation 1 at three stages of its evolution, at the start of the simulation, at the midpoint, and at the end

On the middle and left images of Figure 8 some central nodes can be observed around which the network appears to be centered. To examine this feature we plot the node degree distribution of the final MN on Figure 9. We find a small number of highly connected nodes (hubs) and many less connected ones. One might call this a scale free network, therefore we fitted a power law distribution of the form $P(n) = n^{-\gamma}$, shown on Figure 9. We found the parameter estimate to be $\gamma = 1.236$. Similar distributions can be found when examining final networks of other simulations.

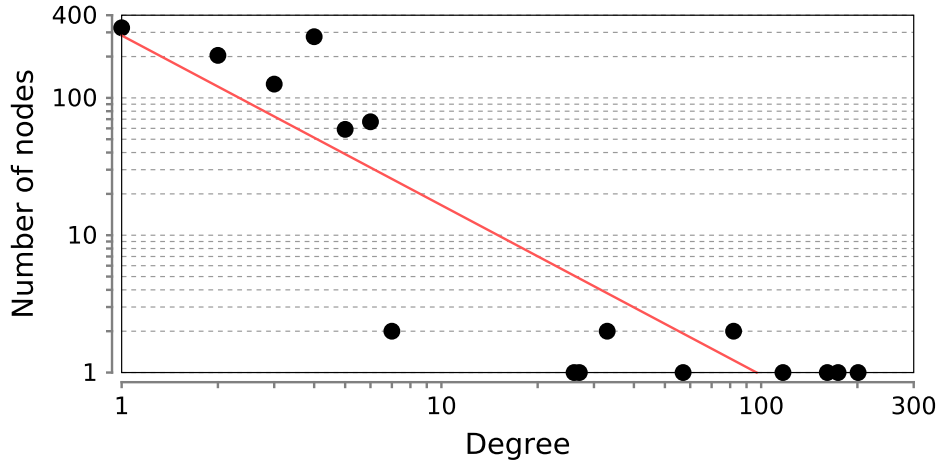


Figure 9: Node degree distribution of the final network of Population 3 of Simulation 1 with a power law distribution fitted

The similarity indices for this simulation are shown on Figure 10, for all the reactions in the MN-s above the diagonal, and for the reactions with nonzero flux below it. Note that in every population we have 100 cells, and therefore in this figure we show $300 \times 300 = 9000$ similarity indices. The used reactions are very similar within the populations, but show a small degree of inter-population similarity. The red and purple stripes in the upper triangular part within Populations 2 and 3 show MN-s that use different reactions from the rest of the population. This is a mutation, either neutral or deleterious, that has spread to part of the population. We know the mutation is not beneficial, as if it was it would appear in the fitness plots of Figure 5, and would quickly overtake the population with a

high probability. When looking at the complete reaction network, the similarity becomes smaller within the populations, and disappears almost completely between populations.

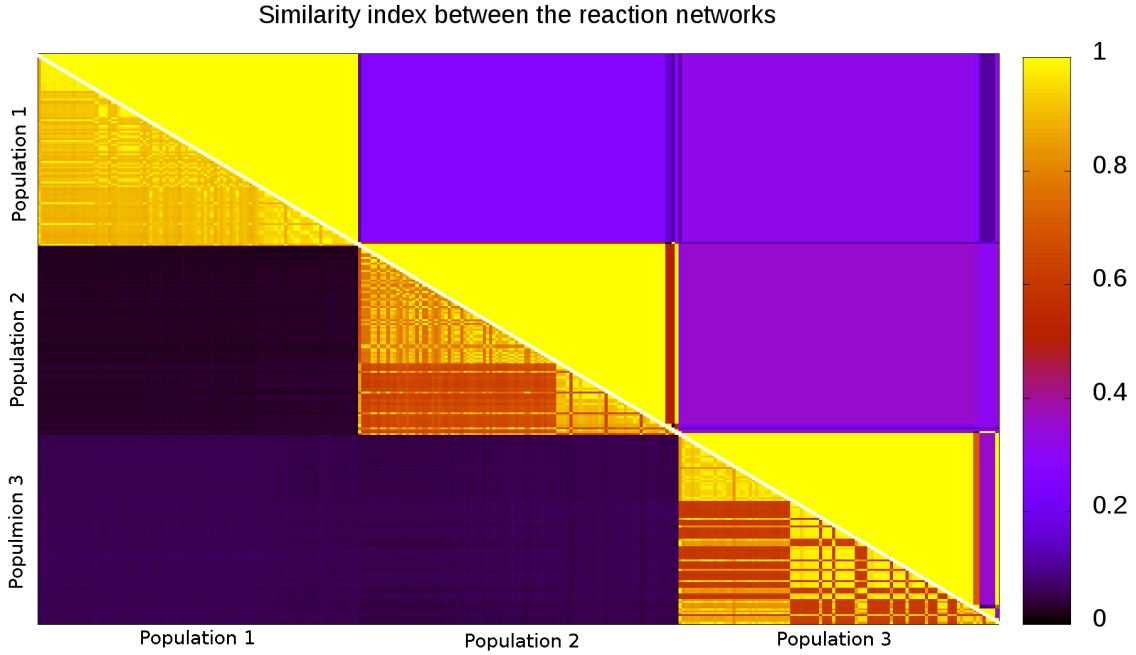


Figure 10: Similarity matrix of the first 3 populations of Simulation 1

The IPR of the similarity indices for every reaction within an MN, comparing each member of 3 populations to the best performing network in the given population is shown on the left of Figure 11 at each of the 10 checkpoints. The IPR of the similarity index for used reactions are shown in the middle of this figure. It shows that the set of reactions within populations is diverse, due to the very high mutation rate, however the used reactions are more similar in a population. The fitness values within a population are very similar, with the exception of Population 3 at checkpoint 6. This outlier value is most likely the effect of the population being overtaken by a mutation at the point of saving the checkpoint. The IPR plots of not shown populations are very similar to the shown ones.

3.1 The effect of mutation rate

The next pair of simulations were run to examine the effect of mutation rates on the patterns of evolution. The initial MN and the objective function of these simulations was the same as for Simulation 1. The probability of point mutation was set to $p_{point} = 0.01$ with the cost of reaction $k_{reaction} = 0.001$ for Simulation 2, and for Simulation 3 $p_{point} = 0.1$ with $k_{reac} = 0.01$. The populations again consisted of 100 cells each, giving the expected number of mutations per generation to be 1 and 10 for Simulations 2 and 3 respectively.

Diagnostic plots for 3 typical populations are shown on Figure 12 and Figure 14.

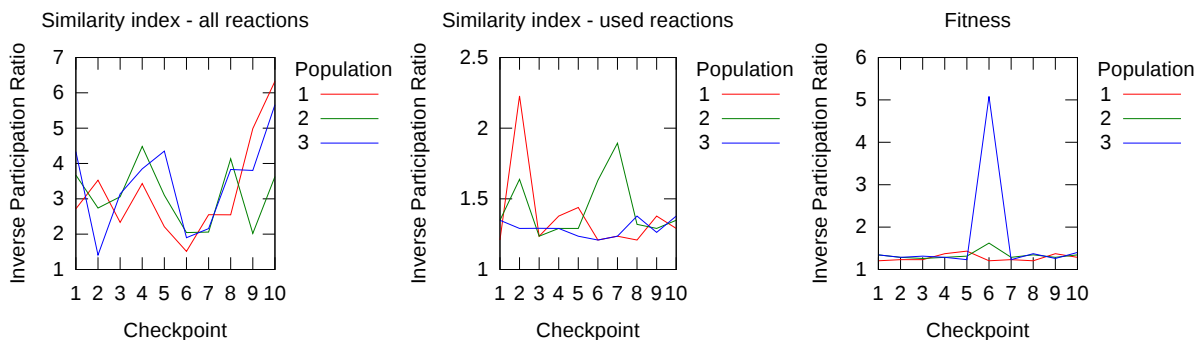


Figure 11: Inverse participation ratio of the two similarity indices and the fitness of 3 population of Simulation 1 at each checkpoint

Both simulations evolved the populations of MN-s for 6×10^7 generations. This meant that Simulation 3 had ~ 10 times more mutations than Simulation 2.

Simulation 2 evolved the populations through approximately 600000 mutations, and of the populations that completed the run $\sim 28\%$ had no improvement in their fitness $\sim 55\%$ had an improvement of ~ 0.5 , and 16% have improved by ~ 1 . The discovery of a new pathway to produce ATP increases the fitness function by 0.5 , but after such an improvement the MN-s usually gather a large amount of unused reactions, in this case about 70 reactions. This lowers the fitness function by $70 \times k_{reac} = 0.07$. The number of unused reactions fluctuates wildly around ~ 110 for a network with fitness ~ 1 , and around ~ 150 for a cell with fitness ~ 1.4 . The number of reactions necessary for a fitness increase is 6 (11 reactions in total), and the other increase could be achieved using an additional 4 reactions (15 reactions in total). Overall $\sim 10\%$ of the reactions are used within a MN. The entropy of the population fluctuates around ~ -360 which can correspond to a population of ~ 80 identical cells, and a few mutants that are different from them. This can be observed on the similarity matrix of the final networks shown on Figure 13. We can see that the populations are homogeneous, with very few different cells even when every reaction is considered (below diagonal). The used reactions are similar between populations 1 and 3. The similarity considering all reactions is very low between the populations. The IPR plots of the populations are similar to those shown for Simulation 1, with even less variation in the case of used reactions. An IPR plot similar to this simulation is shown on Figure 19.

When visualizing the final networks of this simulation pathways similar to those at the end of Simulation 1 emerge. The networks have again "rediscovered" reaction 633, and found alternative pathways to produce ATP. The alternative pathways are longer than the original glycolysis, and in the fittest networks they run in pairs. These pairs of pathways run from DHAP to pyruvate, but they meet at intermediate compounds, in some cases more than once. In some cases we find one of these pathways not producing any net ATP, but they contribute to the other part of the pair by providing nutrients to it (eg. phosphate). When considering the node degree distribution of the resulting networks the results are similar to those shown on Figure 9.

Simulation 3 had 10 times more mutations than Simulation 2. Even though the number of

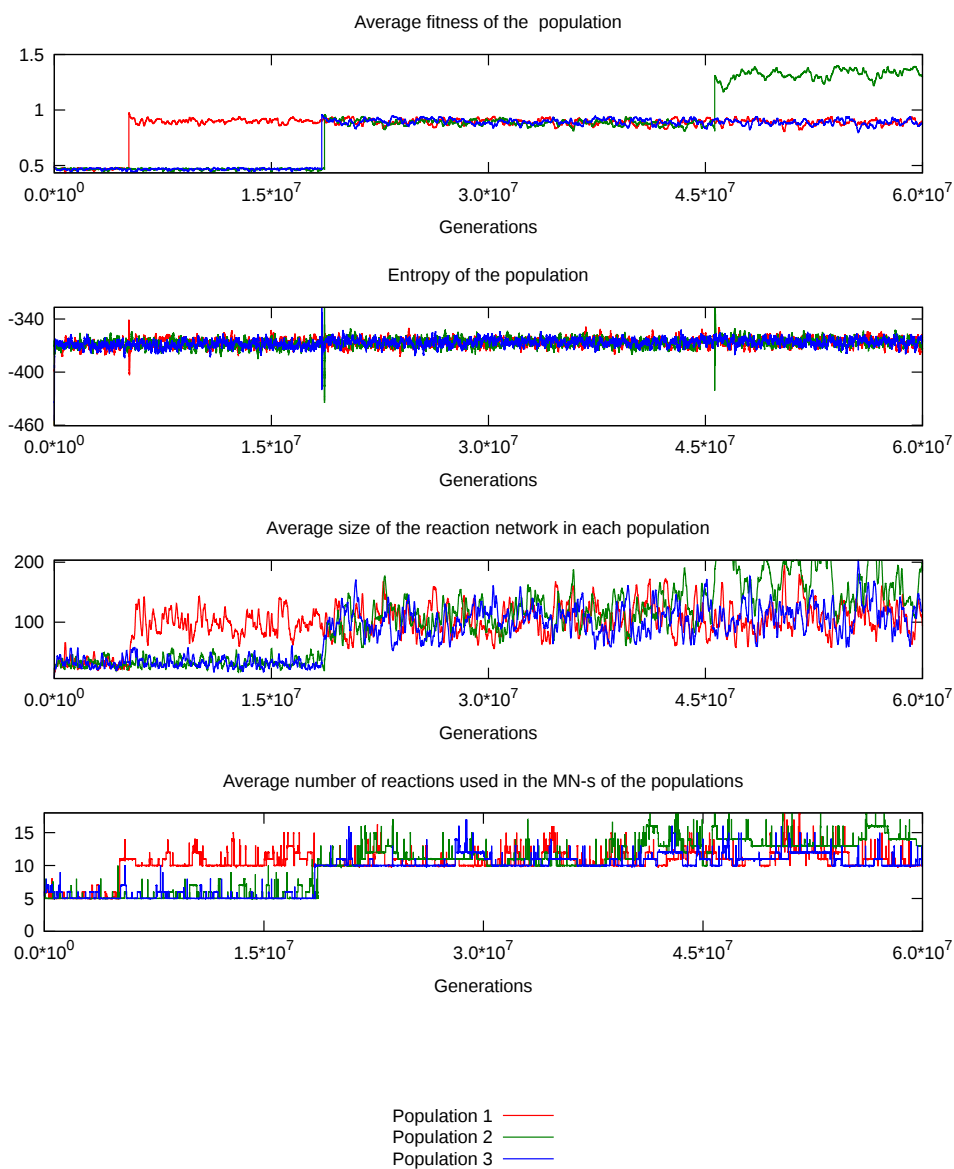


Figure 12: Diagnostic plots of 3 typical populations of Simulation 2

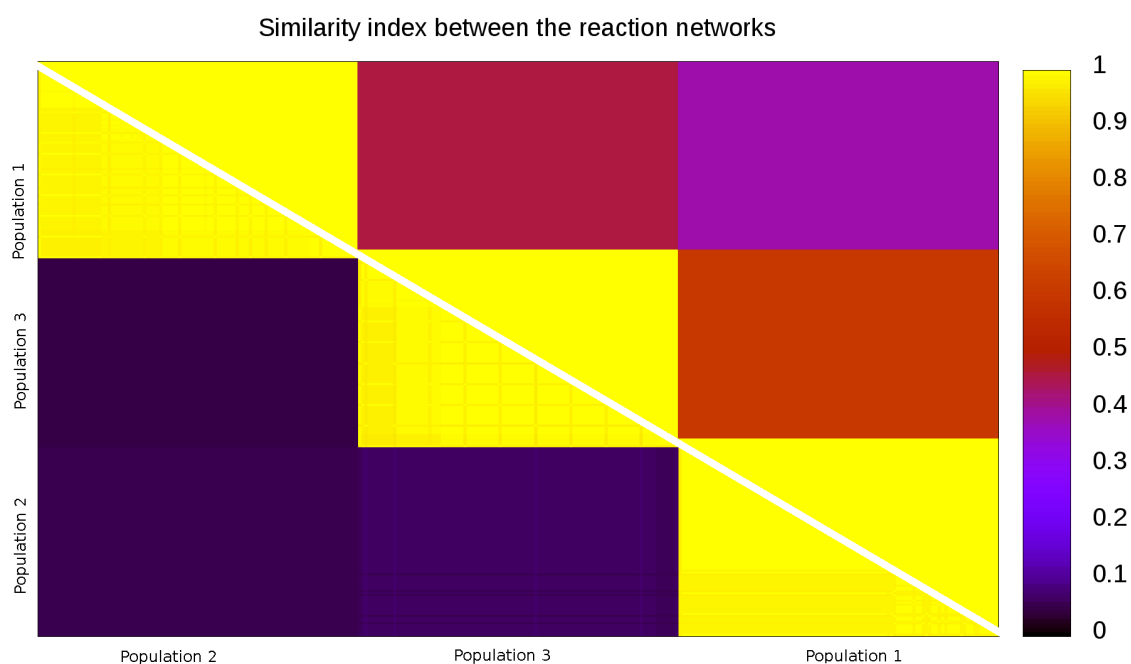


Figure 13: Similarity matrix of the 3 populations of Simulation 2

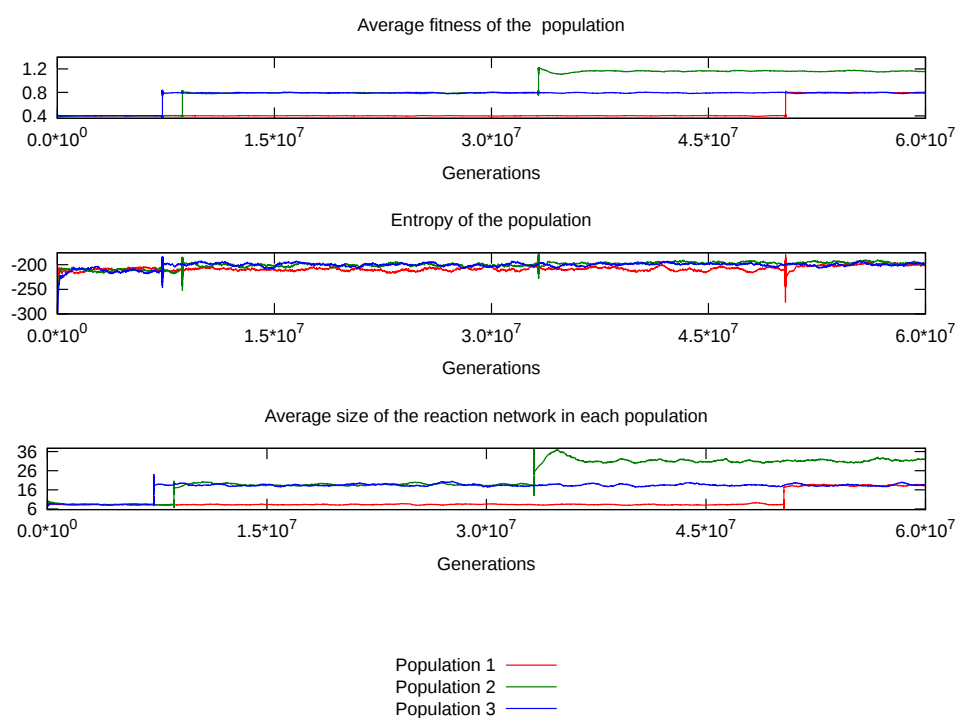


Figure 14: Diagnostic plots of 3 typical populations of Simulation 3

reactions in the MN-s was smaller, due to a higher reaction cost, k_{reac} the populations of Simulation 3 improved further than those of Simulation 2. Here every simulation made advanced their ATP production, $\sim 16\%$ made 1 improvement, 79% made 2, and 5% (1 population) made 3 improvements in their ATP production. After an improvement the networks gain reactions here too, but they only gain ~ 15 networks after a single improvement. The total number of used reactions required for an improvement is similar to that of Simulation 2, but in this case the proportion of reactions used by the MN is $\sim 50\%$. The entropy of the populations fluctuates less wildly than that of Simulation 2, around -200 . This can correspond to ~ 7 approximately equal sized subpopulations, and a few lone mutants. This can be observed in the similarity matrix of the simulation shown on Figure 15. The used reactions are identical within almost every reaction within a population, and they show a rather large degree of similarity between populations too. When considering the whole metabolic network we can see that the populations themselves are diverse, but within a population networks only differ from each other by a handful of reactions.

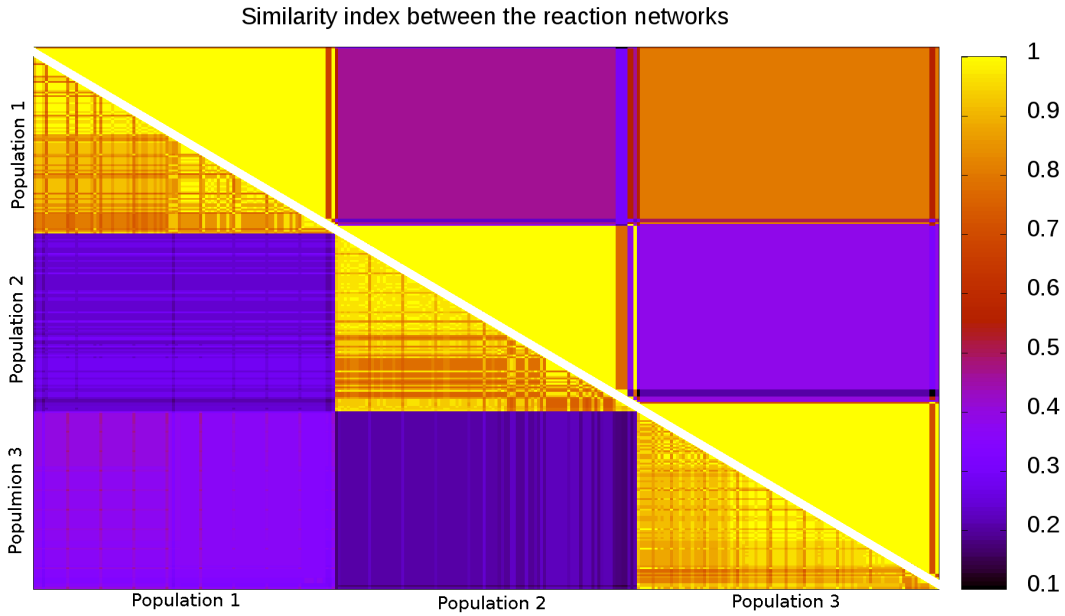


Figure 15: Similarity matrix of 3 populations of Simulation 3.

In an other simulation we have allowed the cells to exchange genetic material (reactions) with each other in a process resembling horizontal gene transfer [30]. A transfer between cells A and B is deemed successful when a randomly chosen reaction from the MN of B is not present in the MN of A, and so can be transferred. After the transfer this reaction is then present in both A and B. When exchanging genetic material we observed that the number of successful horizontal gene transfers was very low ~ 0.01 . The small success rate for this transfer is due to the high degree of similarity within populations, as shown on Figure 15. The effects of horizontal gene transfer could be studied in a simulation setup where two populations evolve separately, with the only interaction between them being a small possibility of horizontal gene transfer between cells in the different populations.

We also considered a simulation with $p_{point} = 0.01$ and $k_{reac} = 0.01$ but none of the 20 populations produced any improvement after a similar simulation time as used above.

3.2 Multiple sources

Real cells import a variety of nutrients from their environment, and most of their MN-s can use multiple similar compounds to produce their end products [1]. To test how the presence of multiple sources influences the process of evolution of our networks, we performed simulations of networks that had access to 2 nutrients. To be able to compare the resulting networks with our previous simulations, the initial network was, as previously, the modified trunk of glycolysis, shown on Figure 4. The two sources used for this network were DHAP as before, and G3P. These two molecules are the end products of the upper glycolytic pathway. They enter the lower part by DHAP being converted into G3P, and the two G3P molecules undergo the same trunk pathway. The sink of the simulation was pyruvate, as before, with the objective function rewarding ATP production only. The simulation was run using $p_{point} = 0.01$ and $k_{reac} = 0.001$. We relaxed the steady state condition on the flux of phosphate, allowing the cell to take phosphate up, or dispose of it. This allows the cell to remove phosphate by other means than the $ADP \rightarrow ATP$ conversion. Interestingly this was not used by the cells. We call this run Simulation 4.

Diagnostic plots for 3 populations are shown on Figure 16. All of the populations that finished the simulation made at least 2 improvements in their ATP production. These first two improvements appeared rather early in the simulation, with the last population to obtain them being Population 2. These two improvements increase the number of used reactions to 10, and the networks acquire ~ 200 reactions in total. Approximately 22% of the simulations made 3 improvements, and 11% made 4 improvements. The number of reactions necessary for the 3 improvement network is 14, and with 17 reactions the system can produce 4 improvements. The entropies of the populations are similar to the previous simulations.

We show one of the fittest networks at the end of this simulation on Figure 17. The network has abandoned the DHAP source, instead using only G3P. This is a phenomena appearing in all the populations. The flux through the reactions is shown on the figure by the different thickness of the arrows. The thinner ones symbolize reactions with flux 0.5, while the thick ones mean a flux of 1. It is important to note how interlinked the network is. While there are 3 pathways leading away from G3P, and there are also 3 leading in to pyruvate, these pathways are very connected. The pathways starting with reaction 883 meets with the one starting with 879 at phosphoenolpyruvate, and the paths starting with 879 and 877 diverge and meet at glycerate.

When comparing the similarity matrices of the populations we find that the diversity within a population is small, much like on Figure 15. The networks with 3 improvements show a large degree of similarity in the used reactions ~ 0.8 . Of those with only 2 improvements, there is a pair where the used reactions are identical, and many of them have a moderate amount of similarity between them ~ 0.6 . If we look at the whole list of reactions, any pair of networks show a very small degree of similarity $\sim 0.1 - 0.2$. This is expected, as the unused reactions are random, their presence or absence provides

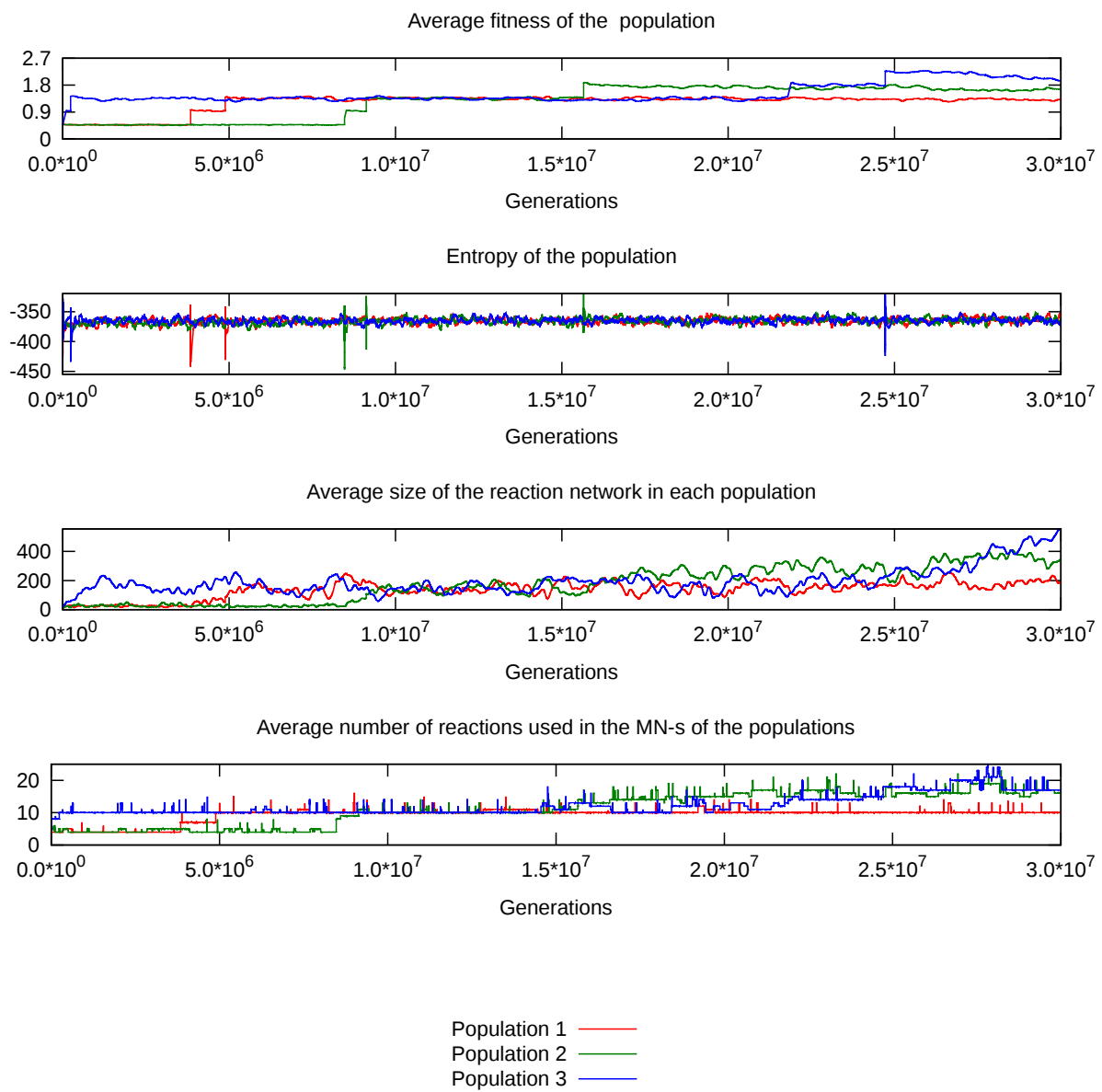


Figure 16: Diagnostic plots for 3 populations of Simulation 4

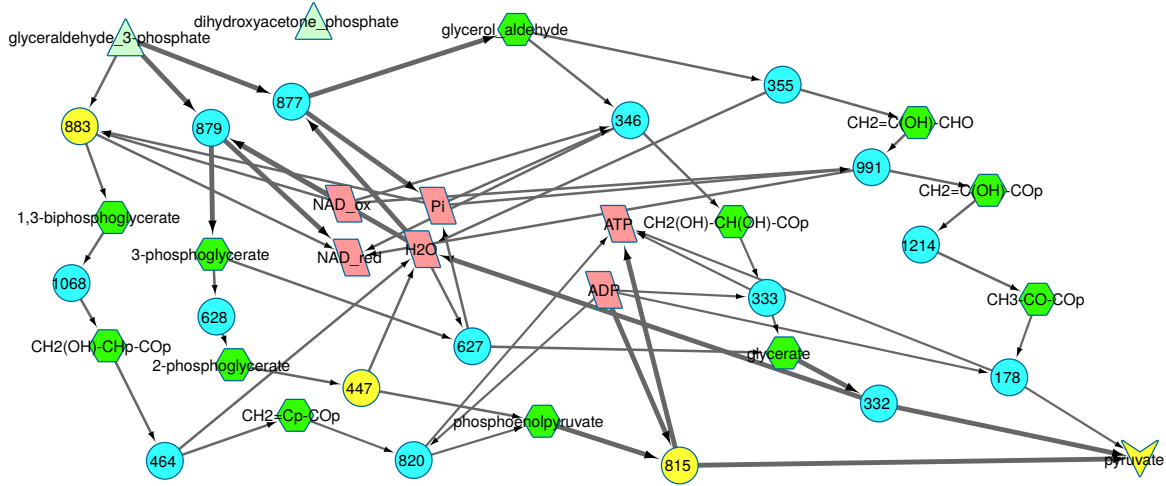


Figure 17: The best performing network at the end of Simulation 4. The reactions used by real glycolysis have been coloured yellow.

no fitness advantage or disadvantage to the cell other than the reaction cost for each reaction. The IPR plots of this simulations are not shown here, as they are very similar to those shown for the next simulation on Figure 19.

3.3 The effect of objective functions

The fitness of real cells is influenced by a variety of factors, including their energy and biomass output. To examine the effects of different fitness functions on their evolution we consider simulations where we reward the cells for a combination of their energy output and their biomass production. Due to the limitations of the linear programming method used in flux balance analysis this combination can only be linear, $f_{goal} = av_{energy} + bv_{biomass}$ for some constants a and b . A more realistic approach could be implemented using non-linear objective functions of the form $f_{goal} = \min(v_{energy}, v_{biomass})$. In this setup the cell would have to produce both energy and biomass, both of which are requirements of reproduction. Such a objective function would be more realistic as the cell needs both energy and biomass for the reproduction. If has a large amount of either, but none of the other reproduction would not happen.

We performed simulations with equal weights for ATP and biomass (pyruvate) production, $a = b = 0.5$ in the above formula, and also ones with only rewarding biomass production ($a = 0, b = 1$). We run these simulations with DHAP and G3P as nutrients separately, and combined too. The results for all three nutrient cases were very similar for the pyruvate only objective function, but the combined nutrient case showed more interesting results for the composite objective function. We present the results of the combined nutrient cases. As the nutrients of the network are phosphate containing, and the sink is not, we allow the network to take up or dispose of phosphate, as in the previous simulation.

Simulation 5 used $p_{point} = 0.01$, and $k_{reac} = 0.001$ as before. The nutrient of the network was G3P and DHAP, and its sink pyruvate, with the rewarded flux in the objective

function being pyruvate production only. We show diagnostic plots for 3 populations of this simulation on Figure 18.

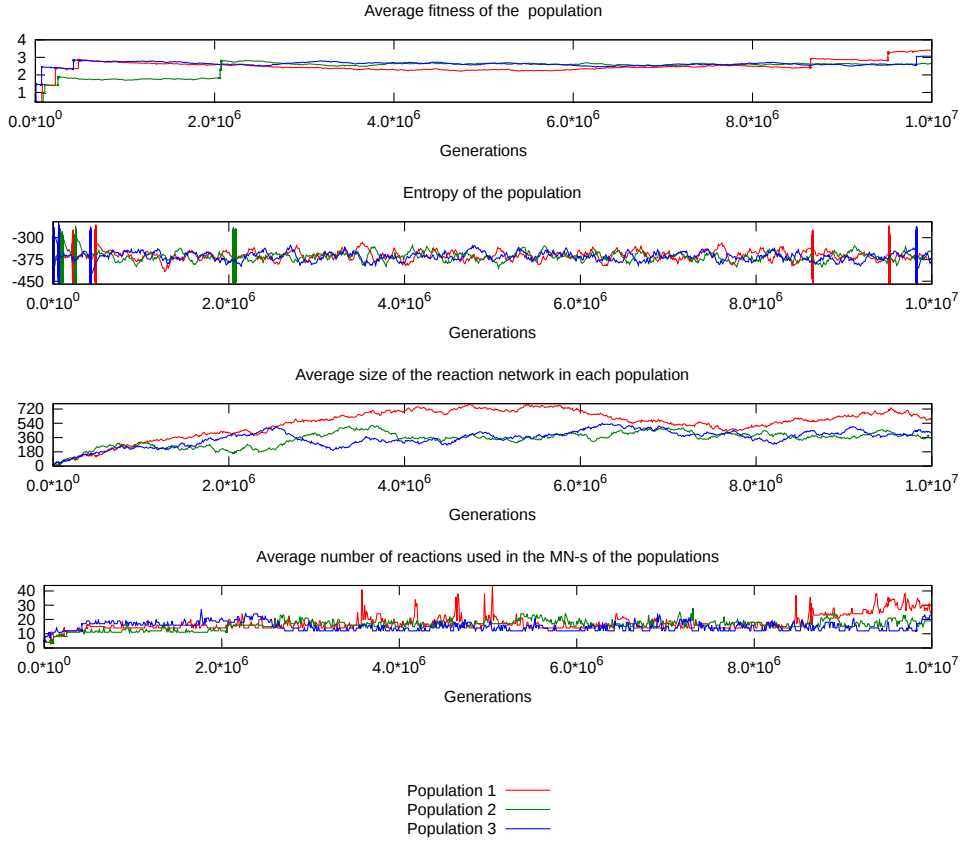


Figure 18: Diagnostic plots for 3 populations of Simulation 5

Even though this simulation only considered 10^7 generations, the networks have made significant improvements very rapidly. Every population achieved a fitness value ~ 2 in the first $\sim 10\%$ of the simulation time. Approximately 15% of the populations made 6 improvements, producing a pyruvate flux of 4, compared to the original 0.5. The reaction networks gain unused reactions after each improvement as seen on the previous diagnostic plots, the networks with the most improvements have ~ 500 reactions at the end of the simulation, giving them a fitness value of ~ 3.5 . The MN-s rate of obtaining new reactions appears to be smoother than for the simulations before, and the number of reactions in the networks fluctuates less. The fittest networks use ~ 30 reactions at the end of the simulation, but Population 1 uses up to 40 reactions at one stage of its evolution. It is interesting to note that the increase in the number of used reactions does not come with a fitness advantage in this case, meaning the network most likely lost a reaction (due to a mutation) and it could find an alternative, but longer path to produce the same pyruvate flux as before. Such a mutation has spread in a population multiple times during the simulation as we can see on the last graph of Figure 18. Closer examination of the log file produced by the population shows that the phenomena doesn't always spread in the population, sometimes it only affects the best cell. We show the IPR plots for the 3

populations on Figure 19. The populations are more similar than those with a higher mutation rate. This can be observed in all three graphs. The populations are almost completely homogeneous in terms of used reactions, and they are more similar (smaller IPR value) in terms of all the reactions and the fitness values.

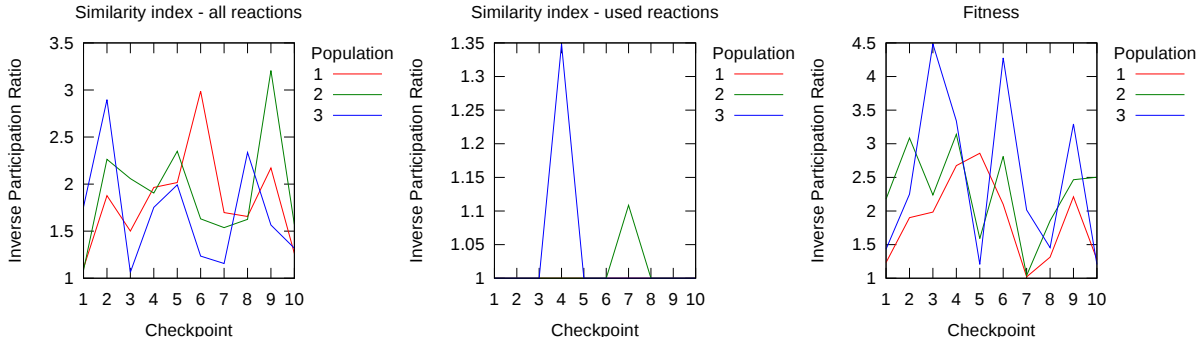


Figure 19: IPR plots of 3 populations of Simulation 5

It is interesting to note that the shortest reaction, discovered by most networks very early, providing twice the original pyruvate flux is only 3 reactions long. One such path is $\text{G3P} \rightarrow \text{3-phosphoglycerate} \rightarrow \text{glycerate} \rightarrow \text{pyruvate}$, with the phosphate being discarded at the middle reaction. As in this case we did not reward ATP production, the networks rather discard the phosphate groups they shed from the nutrient, but some of the networks generally still produce a small amount of ATP, while others consume a small amount.

Most of the populations abandon the DHAP source early in the simulation, and use G3P, as in Simulation 4. Towards the end of the run, the fittest networks return to it, and use a small amount of DHAP. The pathways starting from DHAP are joining into the G3P paths quickly, within 1 – 2 reactions. The metabolite where the two pathways join (eg. $\text{CHO-CO-CH}_2\text{p}$) can be considered a precursor molecule, as it is processed the same way regardless of the source.

Simulation 6 was setup using the same parameters as Simulation 5 except for its objective function, which in this case was an equal weighted combination of ATP and pyruvate production. The simulation has again been run for 10^7 generations. Even though this is shorter than Simulation 2, the networks have shown rapid improvement, and the runtime of the two simulations was approximately equal. This is due to the networks of Simulation 6 growing much larger than those of Simulation 2.

We show diagnostic plots of 3 populations of this simulation on Figure 20. The networks start to improve very early on the simulation, some in the first few thousand generations. The improvement steps were generally smaller than those for Simulation 5, usually bringing an improvement of ~ 0.25 , meaning either ATP or pyruvate production was increased by 0.5. This wasn't always the case, for example Population 1 has a larger jump visible on Figure 20 near the beginning of the simulation. The fittest network of the simulation (in Population 1) had a final fitness value of 3.28. The value of the objective function of this network is 4.25, which is lowered by the network having 967 reactions in total at the end of the simulation. After an improvement we don't see the sudden increase in the number of total reactions, as for the previous simulations, but the networks keep ob-

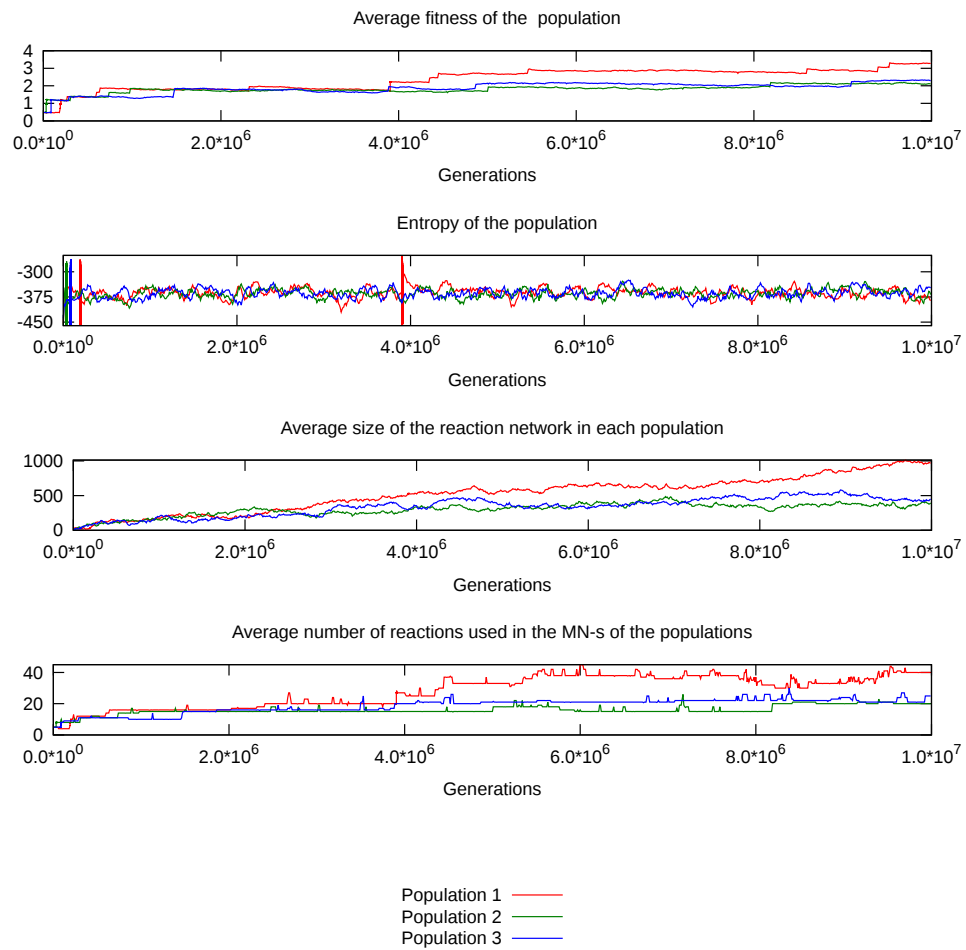


Figure 20: Diagnostic plots for 3 populations of Simulation 6, BETTER PIC IF SIMS FINISH

taining new reactions throughout the whole run. Approximately 11% of the populations improved to a fitness value above 3, $\sim 35\%$ of them to above 2, with the rest of them remaining around 1.8. The fittest reactions collect $\sim 800 - 1000$ reactions, those above 2 have ~ 500 , while the rest 300 – 400. The number of used reactions in the fittest network is 40, those with fitness above 2 have ~ 25 used reactions and the ones with fitness ~ 1.8 have 14. The entropies of the populations show fewer spikes then before. The lack sudden increases in the number of reactions, and the spikes in entropy are most likely the result of the smaller improvements. In this simulation the summary statistics shown on Figure 20 were written out every 10000 generations, unless a larger increase in fitness was observed. Since most of the improvements were ~ 0.25 these have not triggered the writing out of intermittent statistics. The simulation could be run again with lowering the threshold for this trigger, but unfortunately we didn't have enough time for this.

The similarity matrix of the populations show a large degree of similarity within the populations, as before. The inter-population similarity is higher than before, often above 0.7 for the used reactions, and there is 3 populations (of fitness ~ 1.8 that have identical used reactions. These populations have been stagnant at this fitness level for approximately the last third of the simulation, therefore the configuration obtained by them might constitute a local optimum. These networks have 14 – 15 used reactions, while most of those with fitness above 2 have ~ 25 . The networks might have a difficulty in obtaining enough useful reactions to reach the next fitter state.

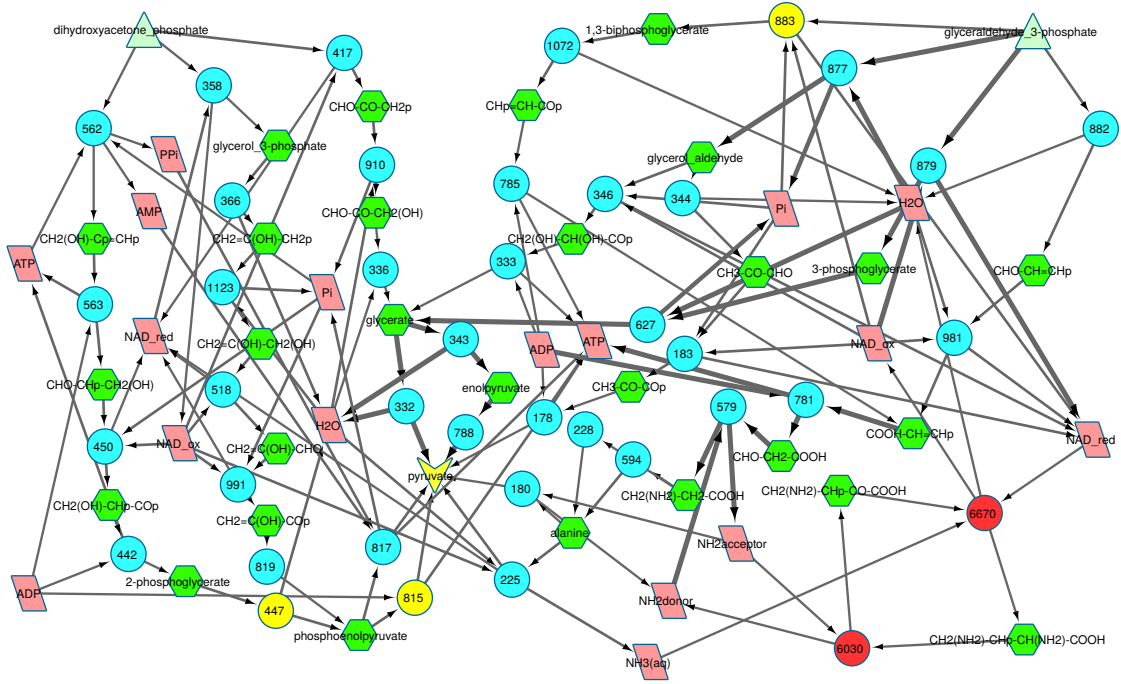


Figure 21: Fittest network of Simulation 6. Reactions from the real glycolytic network are marked with yellow

We show the fittest network of this simulation on Figure 21. This network uses both of the sources it was provided, with the networks connecting the two sources to the sink, connected by only a few reactions. Note that there are multiple instances of certain

internal metabolites on the figure (ATP, ADP, H_2O , NAD^+ and NADH). This was created solely for the purpose of better showing the network, the cell received the same nutrients as before. Should we not have included multiple instances of these, the image would be difficult to interpret due to the large amount of arrows crossing. We show the reactions of the real glycolytic pathway with yellow. An interesting feature of this MN is the cycle marked by red. This pair of reaction takes ammonium and converts it into a source of amidogen (NH_2). This is then inserted on a compound that did not contain nitrogen previously. This amidogen group is removed only at the last step of the pathway, when converting to pyruvate. This set of reactions is a very interesting way of allowing the cell to produce more pyruvate.

4 Discussion

In this work we have considered the effects of the rate of mutation and the objective function on the patterns of evolution in our model. We have found similar evolutionary patterns when we modified the rates of mutation, but improvements appeared later when we decreased it. We found more diverse networks appeared if we used multiple sources, but this might be a result of a poor choice of our original source. When we considered more complex objective functions the number of improvements increased and the resulting networks became even more complex.

The effect of mutation rate

The authors of [34] note that crucial parameters for modeling evolution, such as the frequency of beneficial mutations are not known. The rate of spontaneous mutations per genome per genome replication is approximately 0.01 for higher eukaryotes [10]. We have considered mutation rates comparable to this, but it is important to note that the genome of our organism are very short compared to that of real organisms. High per gene mutation rates such as those we considered can be relevant to very early stages of evolution. Decreasing the mutation rate to a value lower than 0.01 while keeping the population size at $N = 100$ yields no improvements in similar scale simulations as the ones considered above. This is because decreasing the mutation probability (eg. to $p = 0.001$) means the expected number of mutations per generation will be less than one, making the populations too homogeneous for mutations to spread fast enough. If these simulations were run for a considerably longer time than the ones we performed they might show improvements.

We observed similar networks emerging in most of the populations of any given simulation. In the case of Simulations 1, 2, and 3 the emerging networks were similar between simulations too. It would be interesting to see whether every population would arrive to the same network if we allowed the simulations to run for a long enough time. We found that the expected times until an improvement appears within a network increases as the mutation rate decreases. This effect might appear because of the small population size we used. In real organisms the rates of mutations are smaller than in our simulations, but the size of their populations are vastly greater than those we considered. A 1 ml

liquid sample of bacterial colonies can contain bacteria in excess of 10^9 [35].

We find that the fitness cost of reactions also influences the improvement patterns. These costs must allow the network some "experimental" reactions, that are not themselves used, but form a pool of reactions from which improvements can emerge. If the cost of having a reaction is high, the number of reactions is too tightly bound, the network takes more mutations to improve, as we have seen in Simulations 2, 3 and the unsuccessful $p_{point} = 0.01 = k_{reac}$ simulation.

In our model we found no difference in the evolution of the networks depending on the presence or absence of horizontal gene transfer. This is most likely the effect of our very homogeneous populations.

The effect of multiple sinks and different objective functions

When we allowed our organisms to use multiple molecules as sources while keeping the objective function as before we observed the networks abandoning the initial source DHAP in favour of G3P. This influenced the evolutionary patterns shown by the populations by allowing more and faster improvements in the fitness of the cells. This is most likely the effect of G3P being better suited to serve as a nutrient than DHAP, but further simulations with different nutrients would need to be performed to confirm this.

The fittest organisms of Simulation 5 returned to the DHAP source by the end of the simulation. This could mean that the network has reached the maximal flux possible while using G3P only. These networks use DHAP to produce a compound that was already produced by the G3P only network with a smaller flux, using this compound similar to a precursor molecule.

It would be interesting to see whether similar networks using precursor molecules would emerge if we allowed the network to use different nutrients. Precursors would likely emerge in dynamic environments, where the availability of nutrient fluctuates with time. Simulations considering this could be performed using our code with slight modifications to it.

An important difference between the first and second three simulations is that for the second three we allowed our cells to take up or dispose of phosphate. Doing so we observed more diverse improvement patterns; this is a result of our nutrients containing phosphate, while the sinks of the network do not. If we do not allow phosphate to be disposed of, the only way for the cell to rid itself of the phosphate of the nutrient is via the auxiliary reaction $ATP \rightarrow ADP$ ⁷. We have deliberately not included the phosphate to allow the reaction to dispose of phosphate.

When we reward multiple processes in the objective function of cells their evolution can take smaller steps at one time. By allowing them to exchange phosphate with their environment we decouple the process of ATP production from biomass (pyruvate) production. This allows the cells to develop a pathway that does only one of the two goals giving the process greater flexibility. The resulting networks are more complex than previously, with

⁷In the real world this reaction works by consuming a water molecule and producing a phosphate, $ATP + H_2O \rightarrow ADP + Pi$

two lightly connected sub-networks, for the two sources. Such a network could function as a module within the glycolytic pathway providing a high degree of redundancy to it. The upper part of glycolysis produces DHAP and G3P, these could be processed using the network shown on Figure 21. In case of the loss of reactions in either substrates network a larger flux could be used by the other network by using the reaction $\text{DHAP} \rightleftharpoons \text{G3P}$, keeping the performance of the cell intact.

The pair of reactions shown in red on Figure 21 play a role somewhat similar to the citric acid cycle, in the sense that they conserve the carbon containing molecules within themselves and use a circular pathway. In contrast to the citric acid cycle that is driven by the energy releases during the oxydization of pyruvate, our cycle is fuelled by the reduction of the partaking compounds via NAD^+ (Nad.ox on the figure).

4.1 Limitations of our approach

The main limitations of our model arise due to the small population size, the restrictions on the chemistry and the simplifications introduced by using flux balance analysis.

The populations of simple organisms, that our MN-s model are usually substantial. The probability of the fixation of a neutral mutation is inversely proportional to the population size, thus for such large populations it is very unlikely. In our populations with size $N = 100$ approximately one in every hundred mutations fix in the population. This aides the emergence of beneficial mutations, since only a set of unused reactions can contribute to a fitness advantage. For example in Simulation 2 the MN-s need 4 additional reaction to produce more ATP. 3 of these reactions must fix in the population as a neutral one, and stay dormant until the last reaction can fix too. Thus smaller populations might be able to increase their fitness faster than large ones. This claim is supported by [20]. Although we have not examined the effect of population size in our model the program could easily be extended to accommodate a larger population. Existing research suggests that in case of larger populations the patterns of evolution become more deterministic with larger populations [34].

We restricted our cells to use a small but realistic set of possible molecules in their MN-s. As the lower part of the glycolytic pathway only utilizes molecules that are present within our network, this has probably not served as a limiting factor in modeling the evolution of the networks. We have performed test simulations using a larger set of molecules, using CHOPN molecules containing up to 5 carbon atoms. The number of such compounds in our list is 12606, and there are 100835 reactions between them. The results of these simulations were similar to those discussed in Section 3. This is likely the result of our nutrients being 3 carbon molecules. In order for the networks to venture into the set of molecules containing 4 or 5 carbon molecules, they would have to obtain this carbon from the only source of carbon other than the nutrients, CO_2 . The release of CO_2 is an exothermic reaction, therefore its capture would be endothermic, in other words requiring a large investment of energy. While the networks could invest this energy using ATP⁸,

⁸An example for this is reaction 182 in our list of 4 carbon reactions: pyruvate ($\text{CH}_3\text{-CO-COOH}$) + ATP + $\text{CO}_2 \rightarrow$ oxaloacetate ($\text{COOH-CH}_2\text{-CO-COOH}$) + ADP + Pi with $\Delta G_0 = -8.825$ UNITS OF DELTAG

the resulting network would probably not produce a net flow of ATP.

A more important restriction was necessary to make in order to keep the flux calculations a linear programming problem. In such a problem one needs to provide boundaries for the parameters that are to be optimized, in our case the fluxes through reactions. These boundaries can be infinite, and can contain other fluxes, such as $v_1 + v_2 < c$, but can only be linear functions of them. This forced us to determine the direction of every reaction depending only on its Gibbs free energy change. In real chemical pathways only the overall change of the free energy needs to be negative, in other words parts of the path may have a positive ΔG , if the rest of the path compensates for it by having a large enough negative ΔG value. Such a constraint would look like $\sum_{i=1}^N \Delta G(v_i) < 0$, where $\Delta G(v_i) = \frac{-v_i}{|v_i|} \Delta G_i$, with ΔG_i being the free energy change of reaction i . Here $\Delta G(v_i)$ simply flips the sign of ΔG_i if the reaction is happening in the reverse direction, compared to the direction in the list of reactions. Such a constraint is non-linear due to the sign-taking, and therefore incompatible with the linear programming approach. In contrast our path has to have every reaction’s ΔG as negative, (or not very positive for a reduced flux). Paths that require the investment of energy are not impossible in our network. The energy investment usually comes in the form of an $\text{ATP} \rightarrow \text{ADP}$ conversion, such as in case of the reaction shown on Figure 1.

Flux balance analysis as implemented here also assumes that the maximal flux through each reaction can only be one of three cases, as described in Section 2.2. Using smoother maxima here, eg. calculating the maximal flux as a continuous function of the current free energy change could lead to more accurate results. The likelihood of a reaction happening not only depends on the difference of free energy between the initial compounds and the end products, but also on the free energy landscape between these two states. A reaction with a high potential barrier will be less likely to happen than one where the free energy change is a roughly monotonic function.

In all of our simulations with $k_{\text{reac}} = 0.001$ we observed the large number of unused reactions in our metabolic networks. Some of these unused networks are part of the next potential improvement of the network. If the mutation rate is low, and the cost of reactions high the expected time until an improvement becomes very large. We observed this phenomena in the simulation with $p = 0.01$ and $k_{\text{reac}} = 0.01$ that produced no improvements during a similar time that was used for the other simulations. The genetic information of our molecules consists of the reactions they can produce. In a real cell the genetic information serves a variety of functions, including the coding of proteins that catalyse reactions. A large proportion of the DNA of higher eucaryotes does not code proteins, the estimate for the proportion of human DNA that codes proteins is $\sim 3\%$ [38]. This DNA is sometimes referred to as junk DNA, as its function is not well understood. Its purpose can be redundancy, in case of the coding parts of the DNA are damaged. In our network some unused reactions can potentially serve as "backups" in case some of the currently used ones are removed. We would like to have tested this phenomena on the evolved networks, by calculating the fitness of the networks if one or more randomly chosen used reactions are removed. Unfortunately time did not allow this. REPHRASE

Further research in the area could consider the effects of different environmental variables, such as temperature, acidity and the concentration of metabolites. Our code can be easily adapted to use different environments. The effects of sample size could be analyzed by

considering larger populations, with the same mutation rates as we did, however in case of a larger population the mutation rates can be further decreased to closer approximate that of real cells. The evolution of the networks could be examined in a dynamically changing environment, for example varying nutrient availability or physiological conditions. Simple examples of such dynamic environments could be simulated using our software with slight modifications.

Acknowledgements

I would like to thank my supervisor Dr. Bartek Waclaw, for his time and guidance throughout the project; Máté Nagy who provided help and advice in setting up the program, and continued aiding me in resolving difficult bugs; and Ioan-Bogdan Magdau for his code calculating moving averages.

References

- [1] Aditya Barve and Andreas Wagner. A latent capacity for evolutionary innovation through exaptation in metabolic systems. *Nature*, 500(7461):203–206, 2013.
- [2] Aditya Barve, Sayed-Rzgar Hosseini, Olivier C Martin, and Andreas Wagner. Historical contingency and the gradual evolution of metabolic properties in central carbon and genome-scale metabolisms. *BMC systems biology*, 8(1):48, 2014.
- [3] Richard A Blythe and Alan J McKane. Stochastic models of evolution in genetics, ecology and linguistics. *Journal of Statistical Mechanics: Theory and Experiment*, 2007(07):P07018, 2007.
- [4] Béla Bollobás. *Random graphs*. Springer, 1998.
- [5] Balint Borgulya. Evolution of Metabolic Networks. <https://github.com/HoneyMonster7/frankenstein/>, 2015.
- [6] S. J. Court, B. Waclaw, and R. J. Allen. Lower glycolysis carries a higher flux than any biochemically possible alternative. *ArXiv e-prints*, April 2014.
- [7] Charles Darwin. *The origin of species by means of natural selection: or, the preservation of favored races in the struggle for life*. 2009.
- [8] J Arjan GM de Visser and Joachim Krug. Empirical fitness landscapes and the predictability of evolution. *Nature Reviews Genetics*, 15(7):480–490, 2014.
- [9] Peter Dittrich, Johannes C Ziegler, and Wolfgang Banzhaf. Artificial chemistries-a review. *Artificial life*, 7(3):225–275, 2001.
- [10] John W Drake and John J Holland. Mutation rates among RNA viruses. *Proceedings of the National Academy of Sciences*, 96(24):13910–13913, 1999.

- [11] Nathan Entner and Michael Doudoroff. Glucose and gluconic acid oxidation of *Pseudomonas saccharophila*. *Journal of Biological Chemistry*, 196(2):853–862, 1952.
- [12] W.J. Ewens. *Mathematical Population Genetics 1: Theoretical Introduction*. Interdisciplinary Applied Mathematics. Springer New York, 2004. ISBN 9780387201917.
- [13] Iwona J Fijalkowska, Roel M Schaaper, and Piotr Jonczyk. DNA replication fidelity in *Escherichia coli*: a multi-DNA polymerase affair. *FEMS microbiology reviews*, 36(6):1105–1121, 2012.
- [14] Ronald Aylmer Fisher. *The genetical theory of natural selection: a complete variorum edition*. Oxford University Press, 1930.
- [15] Christoph Flamm, Alexander Ullrich, Heinz Ekker, Martin Mann, Daniel Högerl, Markus Rohrschneider, Sebastian Sauer, Gerik Scheuermann, Konstantin Klemm, Ivo L Hofacker, et al. Evolution of metabolic networks: A computational framework. *Journal of Systems Chemistry*, 1(4), 2010.
- [16] Errol C Friedberg, Graham C Walker, Wolfram Siede, and Richard D Wood. *DNA repair and mutagenesis*. American Society for Microbiology Press, 2005.
- [17] C Gyles and P Boerlin. Horizontally transferred genetic elements and their role in pathogenesis of bacterial disease. *Veterinary Pathology Online*, page 0300985813511131, 2013.
- [18] Leland H Hartwell, John J Hopfield, Stanislas Leibler, and Andrew W Murray. From molecular to modular cell biology. *Nature*, 402:C47–C52, 1999.
- [19] Arend Hintze and Christoph Adami. Evolution of complex modular biological networks. *PLoS Comput Biol*, 4(2):e23, 2008.
- [20] Kavita Jain, Joachim Krug, and Su-Chan Park. Evolutionary advantage of small populations on complex fitness landscapes. *Evolution*, 65(7):1945–1955, 2011.
- [21] Hawoong Jeong, Bálint Tombor, Réka Albert, Zoltan N Oltvai, and A-L Barabási. The large-scale organization of metabolic networks. *Nature*, 407(6804):651–654, 2000.
- [22] Judith Kleinfeld. Could it be a big world after all? The six degrees of separation myth. *Society, April*, 12:5–2, 2002.
- [23] Albert Lehninger, David L. Nelson, and Michael M. Cox. *Lehninger Principles of Biochemistry*. W. H. Freeman, fifth edition edition, June 2008.
- [24] Richard E Lenski, Charles Ofria, Robert T Pennock, and Christoph Adami. The evolutionary origin of complex features. *Nature*, 423(6936):139–144, 2003.
- [25] Andrew Makhorin. GNU linear programming kit. *Moscow Aviation Institute, Moscow, Russia*, 38, 2001.

- [26] Makoto Matsumoto and Takuji Nishimura. Mersenne twister: a 623-dimensionally equidistributed uniform pseudo-random number generator. *ACM Transactions on Modeling and Computer Simulation (TOMACS)*, 8(1):3–30, 1998.
- [27] Patrick Alfred Pierce Moran. Random processes in genetics. In *Mathematical Proceedings of the Cambridge Philosophical Society*, volume 54, pages 60–71. Cambridge Univ Press, 1958.
- [28] Nasif S Nahle. Irreversibility.
- [29] Jeffrey D Orth, Ines Thiele, and Bernhard Ø Palsson. What is flux balance analysis? *Nature biotechnology*, 28(3):245–248, 2010.
- [30] Csaba Pál, Balázs Papp, and Martin J Lercher. Adaptive evolution of bacterial metabolic networks by horizontal gene transfer. *Nature Genetics*, 37(12):1372–1375, 2005.
- [31] Nathan D Price, Jennifer L Reed, and Bernhard Ø Palsson. Genome-scale models of microbial cells: evaluating the consequences of constraints. *Nature Reviews Microbiology*, 2(11):886–897, 2004.
- [32] Paul Shannon, Andrew Markiel, Owen Ozier, Nitin S Baliga, Jonathan T Wang, Daniel Ramage, Nada Amin, Benno Schwikowski, and Trey Ideker. Cytoscape: a software environment for integrated models of biomolecular interaction networks. *Genome research*, 13(11):2498–2504, 2003.
- [33] Jeremy Siek, Lie-Quan Lee, and Andrew Lumsdaine. Boost C++ Libraries. <http://www.boost.org/>, June 2000.
- [34] Ivan G Szendro, Jasper Franke, J Arjan GM de Visser, and Joachim Krug. Predictability of evolution depends nonmonotonically on population size. *Proceedings of the National Academy of Sciences*, 110(2):571–576, 2013.
- [35] Bartek Waclaw. The physics of biological evolution. Lecture notes and problem solutions, 2015.
- [36] Heinrich Warburg. Embden-Meyerhof-Parnas Pathway. 2014.
- [37] Duncan J Watts and Steven H Strogatz. Collective dynamics of ‘small-world’ networks. *Nature*, 393(6684):440–442, 1998.
- [38] Kane Ka-Shu Wong, Douglas A Passey, Ying-zong Huang, Zhiyong Yang, and Jun Yu. Is “junk” DNA mostly intron DNA? *Genome Research*, 10(11):1672–1678, 2000.